NASA
Technical
Paper
2335

September 1984

Aerodynamic Design of the Contoured Wind-Tunnel Liner for the NASA Supercritical, Laminar-Flow-Control, Swept-Wing Experiment

Perry A. Newman,
E. Clay Anderson,
and John B. Peterson, Jr.

NASA

NASA Technical Paper 2335

1984

Aerodynamic Design of the Contoured Wind-Tunnel Liner for the NASA Supercritical, Laminar-Flow-Control, Swept-Wing Experiment

Perry A. Newman,
E. Clay Anderson,
and John B. Peterson, Jr.

Langley Research Center
Hampton, Virginia

NASA
National Aeronautics
and Space Administration

Scientific and Technical Information Branch

Preface

This report, the first of a series of publications, is an overview of the numerical procedures used in the aerodynamic design of the contoured wind-tunnel liner for the NASA supercritical, laminar-flow-control (LFC), swept-wing experiment. This information is of general interest to the public and of specific interest to the NASA personnel involved in the present experiment and perhaps in any future redesign of follow-on or related tests. The almost daily advances in computational fluid-dynamic code capabilities and computer technology would certainly require a reassessment of each step in the present design if it were to be used again. The final aerodynamic liner designs for this experiment were completed during 1980 and have been used in the engineering design, fabrication, and installation of the liner in the Langley 8-Foot Transonic Pressure Tunnel. Thus, the purpose of these documents is to record those aspects of the aerodynamic liner-design procedure relating to the overall design strategy and to how the details were accomplished.

Since the aerodynamic liner-design procedure involved the use of a number of computer codes and data-processing steps, it was felt that this first document should present an overview of the entire procedure. Primarily, it indicates what was done, why it was done, the sequence of various steps, and the overall data flow. A condensed version of this overview was presented as AIAA-82-0568 at the AIAA 12th Aerodynamic Testing Conference held in Williamsburg, Virginia, on March 22–24, 1982. The NASA photographs used herein were taken from late 1980 through April 1982 as the liner hardware was being fabricated and installed in the tunnel.

Details relating to how individual steps of the procedure were accomplished or to the use of specific computer codes are to be covered in subsequent reports. These reports will refer to the present report and appropriately identify the procedural steps; the authorship of each will reflect several others who have contributed in this design. The present authors acknowledge the many helpful interactions with a number of persons concerning the technical, economic, hardware, and operational aspects of the NASA LFC swept-wing experiment. In particular, though, we are indebted to Werner Pfenninger, then of The George Washington University, and to Percy J. Bobbitt of the Langley Research Center, for many fruitful technical discussions concerning this aspect of the LFC experiment project.

Contents

Summary

A contoured, nonporous, wind-tunnel wall liner has been designed in order to simulate an unbounded supercritical-flow condition about an infinite-span yawed wing of large chord at low noise and turbulence levels. A swept-wing test panel having a supercritical-airfoil section with laminar-flow control (LFC) spans the tunnel. The numerical procedure developed for this aerodynamic liner design is based upon the simple idea of streamlining and incorporates several existing transonic and boundary-layer analysis codes. A summary of the entire procedure is presented to indicate the design strategy, the sequence of steps, and the overall data flow. The liner is presently installed in the Langley 8-Foot Transonic Pressure Tunnel (TPT) and tests are now underway. The liner-design results given here are examples of the calculated requirements and the hardware implementation of them.

Introduction

The numerical aerodynamic liner-design procedure discussed herein was developed in order to meet the special requirements of a laminar-flow-control (LFC) swept-wing model. A transonic interference-free test condition is needed in order to establish the compatibility of an active LFC wing-suction system with the current high-performance supercritical-airfoil technology. The required very large model chord and the inadequacy of a conventional noisy slotted- or porous-walled transonic test section also necessitate a streamline-contoured, nonporous test section. The test is being conducted in the Langley 8-Foot Transonic Pressure Tunnel (frequently referred to herein as the 8-ft TPT), which has been modified for improved flow quality by the addition of a honeycomb and screens in the settling chamber. An overview of the entire experiment is available (ref. 1) so that only those aspects influencing the liner design will be reported here.

An outline of the design-procedure concept and its application to some initial inviscid "test-section" lines intended for the Ames 12-Foot Pressure Tunnel were discussed in reference 2. A check on the validity of the procedure was provided by a direct comparison of an analytically determined tunnel-wall shape with one determined experimentally in streamlined two-dimensional tunnel tests. These results were given in references 2 to 4, and no further comparisons have been made. A summary of the material given in the present paper is available as reference 5.

The present paper outlines the procedure used in the aerodynamic design of the shape for the entire 8-ft TPT liner. This liner, which is about 54 ft long, extends from within the existing contraction cone, through the test section, and into the diffuser. A simplified schematic of the LFC test setup in the 8-ft TPT is shown as figure 1. The liner has been constructed and installed, LFC model testing has begun, and preliminary results indicate that the liner is performing as intended.

Symbols

CQM	magnification of suction-coefficient distribution in model turbulent region from that in model laminar test region
C_p	pressure coefficient
C_q	suction-coefficient distribution in liner end plate
c	model chord, ft
c_l	section lift coefficient
I	streamline-curve parameter, $x_\perp$ grid index
JI	streamline-curve index, $y_\perp$ grid index
M	Mach number
R_c	Reynolds number, based on chord c
s	nondimensional distance along streamline
t/c	model thickness-chord ratio
U, V, W	nondimensional Cartesian velocity components of 3-D contraction (tunnel coordinates) in figure 6
u, v, w	nondimensional Cartesian velocity components for axisymmetric nozzle flow (tunnel coordinates) in figure 6 and for yawed-wing flow (2-D plus sweep) in figure 3
X_M, Z_M	model planform coordinates (see fig. 16)
x, y, z	Cartesian tunnel coordinates; x along flow axis, y across tunnel, and z up
β_{flap}	model flap deflection, deg
Δ^*	equivalent displacement correction due to viscous and suction effects; see discussion of code CMFLUX in appendixes A and C
Δh	choke-height displacement, depicted in figure 13(a)
$\delta u, \delta v, \delta w$	nondimensional Cartesian velocity components of model flow perturbation in contraction region (see fig. 6)
Λ	model sweep, deg

Subscripts:

$\perp$	section property in plane normal to wing leading edge (i.e., the 2-D section plane)
∞	free-stream property

Abbreviations:

BE	bottom end plate
L.E.	leading edge
LFC	laminar flow control
MAG	magnetic
N. C.	numerically controlled
STC	stream-tube curvature code
SW	sidewall
TE	top end plate
T.E.	trailing edge
TPT	transonic pressure tunnel
1-D,2-D,3-D	one-, two-, and three-dimensional

Liner-Design Concept

The concept of "streamlining" wind-tunnel walls to alleviate tunnel interference at transonic-flow conditions is not new; however, analytical tools needed for realistic implementations of it are only now beginning to be applied. Streamlined liners have been used before in tests of large-chord LFC models at low speeds (ref. 6). The special requirements of the NASA supercritical, LFC, swept-wing experiment seem to dictate a similar approach using transonic-flow theory if one is to produce the desired high-speed flow conditions. Specifically, one desires a proper simulation of an unbounded supercritical-flow condition about an infinite-span yawed wing of large chord at low noise and turbulence levels.

Special Requirements of Experiment

A transonic test condition is needed in order to establish the compatibility of an active LFC wing-suction system with the current high-performance, supercritical-airfoil technology. Airfoil designs for LFC applications have been reported in references 7 and 8; some comparisons of numerical results are given in reference 9. The design concept of the supercritical LFC airfoil to be used in this experiment is described in reference 8. The airfoil shape and design-point (test) conditions, which are required as input to the present liner-design procedure, are given in reference 1 and summarized in the next section.

The LFC experiment must be done in a wind tunnel which has levels of stream turbulence and acoustic noise approaching those of flight conditions so that the suction required to maintain laminar flow on the model is realistic. Conventional slotted- or porous-walled transonic tunnels are inadequate in this regard, as revealed by flow-quality measurements which have been made in the original 8-ft TPT (refs. 10 to 13) prior to installation of screens and honeycomb. However, it was also demonstrated (refs. 10 and 12) that closing the slots and choking the flow at the downstream end of the test section significantly reduced pressure fluctuations in the test section. As already mentioned, reduction of stream turbulence levels in the onset flow will be provided by the honeycomb and five screens in the settling chamber. Design considerations for flow-quality devices (ref. 1) and evaluation of the screen-honeycomb configuration to be used in the 8-ft TPT are given in references 14 to 16 and were done independently of the present liner design.

Transport aircraft presently envisioned for LFC applications have moderately swept wings of high aspect ratio where crossflow instability is the dominant transition mechanism. Consequently, this instability must be investigated at appropriate flight crossflow Reynolds numbers (ref. 1). This requirement, together with the physical-size limitations set by slot-duct construction in the test panel and the required limitations on roughness-height Reynolds number for laminar flow, results in a large-chord swept-wing panel. In the 8-ft TPT both the resulting ratio of tunnel height to model chord and the wing-panel aspect ratio are somewhat less than unity.

Liner Characteristics

The liner designed and constructed for the LFC experiment is characterized by its contoured shape of nonporous materials which produces a specified flow at the fixed transonic design or test condition. In order to produce a transonic wind-tunnel flow which simulates free-air flow about an infinite-span yawed wing, one must contour all bounding test-section walls. This contouring must extend well into the existing tunnel contraction and diffuser in order to establish the flow and minimize loss of tunnel performance. The sensitivity of high-speed channel flows to the effective cross-sectional area-ratio distribution requires that viscous boundary-layer displacement corrections also be made.

The nonporous liner will alleviate the noise caused by the slotted test-section wall of the 8-ft TPT (ref. 10). Some liner suction, however, will be required for wall boundary-layer control because of the presence of the model pressure gradients, especially at off-design conditions. A two-walled choke, whose height can be remotely controlled, has been included in the liner so

that a sonic throat can be established at the downstream end of the test section (ref. 1). As previously observed (refs. 10 and 12), such a device quiets the test section by blocking the upstream propagation of diffuser and drive-fan noise. The liner is designed for a given airfoil configuration at a fixed test condition. Some adaptability—via use of shim strips on and the limited suction in the liner—is available for limited blockage control; in addition, model angle of attack and flap settings can be adjusted to modify the pressure distribution and lift. The complexity, cost, and operational uncertainty of a truly adaptive 3-D wall eliminated it from consideration early in the project. The fixed model-design test conditions used as input for the liner design are as follows:

$$M_\infty = 0.820$$

$$\Lambda = 23°$$

$$c = 7.07 \text{ ft}$$

$$R_c = 20.2 \times 10^6$$

or, in the plane normal to the wing leading edge (2-D):

$$M_{\infty,\perp} = 0.755$$

$$c_\perp = 6.508 \text{ ft}$$

$$R_{c,\perp} = 17.1 \times 10^6$$

$$(t/c)_\perp = 13.0 \text{ percent}$$

$$c_{l,\perp} = 0.550$$

$$\beta_{\text{flap},\perp} = 0°$$

Design Approach

Given the LFC test requirements and desired liner characteristics, the design approach used was as follows: (a) develop a concept for the aerodynamic design of the entire liner, (b) translate that concept into a computational procedure, (c) perform the liner aerodynamic design, and (d) process liner data for fabrication requirements. The design of the quiet, streamlined test section, which was faired into the existing tunnel circuit, is accomplished for this yawed-wing simulation by using available analysis codes for 2-D and axisymmetric inviscid transonic and boundary-layer flows. Data files describing the liner shape and flow conditions are transferred from code to code in the procedure.

This procedure is mechanized but not automated since, at several steps, iterations of input parameters are required to meet design constraints. Furthermore, several global iterations were required in the present application because of the large-scale model, its upstream location in the tunnel, the relatively large supercritical-flow regions, the increased tunnel-contraction ratio, and mechanical constraints. In the present liner design, these global iterations occurred as the procedure was being developed and debugged; in fact, some aspects were frozen early in time because of hardware lead-time requirements and thus became constraints for the remainder of the design process. The final liner-shape data were generated to allow direct postprocessing into tapes for numerically controlled milling machines.

Liner-Design Procedure

The liner-design procedure is based on the simple idea of streamlining and the use of several existing computational tools which make the design of streamlined walls feasible. In this procedure, one (a) determines bounding streamlines in the desired flow in order to establish an inviscid "test-section" shape, (b) extends and fairs these lines into the original upstream tunnel contraction, (c) assesses all viscous blockage corrections in the presence of the model pressure field and required mass removal (suction), and (d) fairs the corrected lines into the original downstream tunnel diffuser and designs a choke shape. These steps are outlined in figure 2 where the output data to be used in the engineering design and fabrication of the liner are indicated at the right-hand side.

For supercritical-flow conditions, an inviscid transonic analysis code was used in order to determine the desired flow field and bounding streamlines. In order to account for the blockage due to viscous effects on the liner, a finite-difference boundary-layer analysis code was used along the bounding streamlines with edge conditions determined by the local flow properties. An axisymmetric (and 2-D) stream-tube code was used in the design and analysis of the upstream contraction shape and the downstream choke contour. A number of other codes were written to prepare, transfer, interface, and manipulate the large data base involved. A more detailed breakdown of the tasks shown in figure 2 indicating the computer codes and data flow between them is given in appendixes A and B, respectively.

The liner designed by using this procedure is for a given airfoil configuration at a fixed design-point condition. The procedure, however, has a general utility which is restricted by limitations in the current ability to calculate the viscous flow field about arbitrary configurations. The design procedure is, of course, directly applicable to the two-dimensional streamlined tunnel problem, that is, the prediction of the tunnel-wall shape and sidewall suction distribution required to simulate free-air flow about an airfoil. An analysis for one 2-D adaptive-wall test is reported in references 2 to 4.

Inviscid "Test-Section" Shape

The supercritical, LFC, airfoil design work discussed in references 7 to 9 employed the 2-D transonic analysis code (Program H) developed at New York University (NYU), as described in reference 17. The present liner-design procedure commences with a 2-D transonic airfoil solution for the velocity field throughout a Cartesian grid plane normal to the leading edge, as indicated in figure 3(a). This was obtained from Carlson's full-potential-equation, 2-D airfoil code TRANDES (ref. 18). The grid resolution in TRANDES near the tunnel walls, upstream and downstream of the model, was deemed to be better for the liner design. However, the Cartesian grid and boundary conditions of the TRANDES code do not resolve the flow details properly around the blunt leading edge of an airfoil (as is done in the NYU code solution). This resulted in a smaller expansion and, thus, smaller lift and supersonic-flow region for the present LFC airfoil. Therefore, the grid parameters were adjusted slightly in the TRANDES code until both the lift and supersonic-flow region agreed reasonably well with those obtained from the NYU code, since this latter code was used in the LFC airfoil-section design. It should also be noted here that the TRANDES code is based upon a nonconservative formulation of the full-potential equations; and when shock waves are present in the flow field, this formulation may not properly represent the streamline shapes (ref. 19). However, since the present design test condition is a shock-free supercritical flow, the streamline shapes are not distorted because of the nonconservation of mass at the shocks.

In order to produce the flow field appropriate for an infinite-span yawed wing, a constant sweep-velocity component w was added as shown in figure 3(a). Integration in the resulting 3-D velocity field, starting far upstream with an initial set of y values (denoted by the dots in figure 3(b)), produces the streamline filaments from which the inviscid "test section" is formed. Note that for a swept-wing flow with lift, the streamline which splits at the leading edge and wets the upper and lower model surfaces remains displaced from itself in the spanwise direction at the trailing edge. Thus, the contoured liner will have steps in the end plates, downstream of the model trailing edge. A streamline assembly program forms the inviscid liner shape by translating these streamline filaments (space curves) according to sweep theory. The liner shape is defined by 144 streamline filaments, 48 each in the top (ceiling) and bottom (floor) end plates and 24 each in the two sidewalls facing the wing surfaces. This is shown schematically in figure 3(c).

An indication of the relative size of the original 8-ft TPT, the LFC model, its embedded 3-D supersonic-flow regions ($M > 1$), and the inviscid liner shape around the model is shown in figure 4. It can be seen that the ratio of liner height to model chord is about 1; there is a little less than 0.7-chord clearance "above" the wing upper surface to the east liner wall with about 0.3-chord clearance "below" the lower surface to the west liner wall.

The final program in this step interpolates these assembled curves onto a grid which is fixed in the tunnel in order to define the ordinates for starting the upstream integration through the contraction section. This latter program also draws pictures of the test-section lines (such as those shown in fig. 4) and performs other appropriate data processing.

Contraction Shape

The procedure for the contraction-section design had to account for a more rapid contraction than that of the existing 8-ft TPT, a cross-sectional shape change from circular to squarish with rounded corner fillets, and a shape perturbation to simulate the upstream free-air model influence on flow direction. The increased tunnel contraction ratio with the liner installed, the requirements for a choke at the downstream end of the test section, and a need to minimize the tunnel-wall boundary-layer thickness (and thus the turbulent regions on the model) result in a very forward location of the model in the tunnel. In fact, the wing panel is located upstream of the original slotted test section. Thus, a shorter nonsymmetric contraction is required in order to simulate properly the flow just ahead of the model.

In the design and assessment of the contraction fairing, extensive use was made of the General Electric stream-tube curvature (STC) code. (See refs. 20 and 21.) A short rapid-contraction axisymmetric nozzle was designed for minimal Mach number overshoot along the wall and little variation in Mach number across the exit plane (at the design test conditions) subject to the 8-ft TPT size constraints. Figure 5(a) depicts the rapid-contraction, axisymmetric-nozzle stream tubes and grid as obtained from an STC code solution. The original 8-ft TPT equivalent radius is superimposed in figure 5(a) for comparison. The asterisk (*) at the downstream end denotes the equivalent radius of the inviscid "test-section" liner at the contraction/test-section match plane, the 36-ft tunnel station. The asterisk upstream denotes the maximum 8-ft TPT radius. The same axisymmetric-nozzle stream tube passes through both points in order to enforce overall mass conservation. The region where the outermost stream tube coincides with the existing tunnel radius is at the plane where the liner is faired into the original tunnel contraction, the 24-ft station. It can be seen that the radial extent of this nozzle velocity field is greater than the

equivalent liner radius (*) at the downstream end of the contraction. The axial extent of this velocity field needed for the liner-contraction design is from just upstream of the 24-ft station to just downstream of the 36-ft station.

Axisymmetric flow velocities are known from the STC solution at the grid points (mesh intersections) shown in figure 5(a). Both coordinate and velocity values are first interpolated onto a cylindrical grid and, from there, onto the 3-D Cartesian tunnel grid. Figure 5(b) illustrates the plane of this latter grid at the 36-ft station; shown are the outer boundary of the region where nozzle flow data are known (depicted by dots), the original 8-ft TPT equivalent radius (depicted by a solid line), and the equivalent liner radius (depicted by a dashed line).

Model perturbation velocities appropriate to the desired free-air flow ($\delta u, \delta v, \delta w$) are determined during the inviscid test-section design and are added to the rapid-contraction axisymmetric nozzle velocities (u, v, w) as depicted in figure 6(a). This is done on the large 3-D Cartesian tunnel grid, two planes of which are indicated schematically, in this figure. The resulting 3-D velocity field (U, V, W) is, of course, no longer axisymmetric.

Integration in this 3-D velocity field is carried out in the upstream direction starting from an initial downstream shape, appropriate to the inviscid test section at the match plane, as indicated by the dots in figure 6(b). The resulting lines (streamline filaments) do not generally intersect the original 8-ft TPT contraction wall and are faired into it at or downstream of the 24-ft station, where the original tunnel contraction is about conical. Cubic spline fairings were used along each filament, and the distance over which this fairing occurred was determined iteratively. That is, for a given length of fairing, the axisymmetric equivalent of the 3-D nozzle was analyzed with the STC code to assess the flow smoothness, adverse wall pressure gradients (Mach number overshoots on wall), and exit-plane flow uniformity. The 3-D nozzle shape is taken to be the inviscid 3-D liner-contraction shape.

Viscous and Suction Displacements

Corrections for both viscous and suction displacements on the liner were determined along streamlines by using the 2-D finite-difference boundary-layer code discussed in references 22 and 23. A number of modifications had to be made for this specific task and some of them are outlined in reference 24. A two-dimensional boundary-layer analysis was deemed reasonably appropriate for all streamlines forming the liner contour except those near the airfoil-liner junction, since outside of this region the streamline curvature-induced cross-flow velocity components along the liner wall should be small. The flow in the immediate vicinity of the airfoil-liner junction is three-dimensional and is to be controlled by applying variable suction rates on both the liner wall and the airfoil surface. Thus, the coordinates defining the physical liner surfaces are the inviscid liner coordinates plus the viscous displacement correction, or an effective displacement correction (ref. 25) if surface mass transfer is applied along streamlines.

A 2-D boundary-layer solution was obtained along each of the 144 stream filaments which form the inviscid liner shape. As indicated in figure 7(a), these integrations started far upstream in the contraction and stopped downstream well beyond the test section. These integrations were done in the presence of the desired model pressure field; and around the model junction, suction levels were automatically determined to prevent the turbulent liner boundary layer from separating. The required equivalent displacement correction (i.e., viscous plus suction contributions) was calculated as a relative effective deficit stream-function correction downstream of a reference plane which was taken near the end of the contraction region where the boundary layer is thin. This deficit stream-function-correction concept is discussed in appendix C.

A wedge-shaped region of turbulent boundary-layer flow develops on both model surfaces because of the turbulent liner end-plate boundary layer. Corrections for both viscous and suction displacements (blockage) due to the presence of these regions were also determined by using the 2-D boundary-layer code of references 22 to 24 as effective deficit stream-function corrections. On each of the four wing-surface regions (i.e., upper and lower surfaces at top and bottom end plates), 66 streamline integrations were made as indicated in figure 7(b). The resulting displacement correction, which has a spanwise dependence, could not be applied by modifying the model coordinates (because of the construction cost); instead, it was applied by modifying the liner end-plate displacement correction as indicated in appendix C. Downstream of the model trailing edge, these same streamlines lie either on the liner step or in the viscous wake. The calculation of the turbulent boundary layer along each streamline is appropriately continued downstream of the trailing edge, and the resulting blockage corrections for both the viscous wake and liner-step turbulent boundary layer are also taken into account in the liner.

Diffuser and Choke Fairings

The increased tunnel contraction ratio, due to the presence of the liner and the need for a choke at the downstream end of the test section, requires additional length downstream of the model in order to diffuse the flow smoothly while fairing into the original tunnel diffuser. Since the choke would not be swept and the top and bottom liner end plates contained the

nearly vertical steps downstream of the model trailing edge, it was decided to choke the flow with a two-wall, remotely variable choke device (plate) on each of the approximately vertical sidewalls of the liner.

The test-section liner shape was determined downstream of the model trailing edge, and both diffuser and choke fairings were based upon these extended test-section lines. First, a smooth fairing was obtained between the model trailing edge and the beginning of the choke contour by slowly changing the liner cross-sectional shape while retaining the cross-sectional areas from the extended test-section liner. Downstream of the choke leading edge, the shape and area were slowly changed to fair smoothly into the original tunnel diffuser shape (and area). Next, choke contours were designed by using third-order polynomial curves at the downstream end of the test section. Calculations for the equivalent area distribution were made by using the STC code (refs. 20 and 21) to analyze the flow over the choke; some of the procedural details are given in reference 26. The variable choke-height deflections incorporated in the hardware are sufficient to choke a uniform upstream flow for Mach numbers between 0.80 and 0.84.

Liner Data Flow

The flow of data within the aerodynamic liner-design procedure outlined previously is indicated by the arrows between the major tasks in figure 2. Details of the data flow between programs within these major tasks are given in appendix B. The liner shape is generated as 144 parametric space curves (streamline filaments) and is transferred within and through the aerodynamic design procedure as data files (logical tapes) stored at the Langley Research Center in the Control Data CYBER 175 computer systems. The suction data for the wing turbulent-wedge region and liner end plate are also generated as and transferred via computer data files.

The final step in the liner-design procedure is to process the data so that they can be put into a format suitable for engineering and fabrication purposes. The flow of data files and information for the final liner shape is given schematically in figure 8. The entire previous discussion on the aerodynamic design procedure concerns what was done to generate the data files denoted by the small block labeled "aero liner-design files/data" at the upper left of figure 8.

Liner-Hardware Concept

The hardware implementation of the aerodynamic liner design has imposed a few constraints on the design procedure; thus, it is appropriate here to say simply what the concept was. The liner-hardware design and fabrication have been completed. Throughout most of the tunnel, the liner is composed of rather rigid foam material bonded to a 3/4-in. plywood backing. The liner was divided into about 100 blocks that were machined on a large numerically controlled milling machine and then fitted with pressure taps where specified. Photographs of a sample liner block being fabricated and of a completed one with mounting holes and pressure taps installed are shown as figure 9.

These blocks are mounted on a liner substructure to which studs have been welded; the substructure itself is attached to the original tunnel walls. Figure 10 shows the substructure under the liner-contraction fairing at two successive stages of installation. Figure 11 shows upstream and downstream views of the substructure through the test section and choke regions of the liner. Fabrication inaccuracies in the stream-tube area defined by the liner should be primarily those due to the substructure and liner-block joint finishing, since the numerically controlled milling of the liner blocks can be done to very close tolerances.

Liner-Design Results

At a number of steps within the design procedure previously outlined, many iterations were required in order to satisfy the constraints imposed by the original tunnel walls and the liner configuration required to produce the desired model flow field. In addition, several global passes through the entire procedure were also made as the final LFC airfoil evolved. Some of these early applications of portions of this procedure were made to assess the following: model sizing and location within the tunnel, compatibility of test conditions and size constraints, longitudinal extent of liner and compatibility with the original tunnel, and generation of approximate liner shapes for long lead-time engineering concept studies. The liner-design results given subsequently are representative of those from the final pass through the design procedure and, as such, represent what was used in the hardware design.

Aerodynamic Shape

Views of the final liner shape for the contraction, test section, and diffuser are shown in figures 12 to 14, respectively. In each of these figures, part (a) is an upstream view through line drawings of several cross sections for the stream tube defined by the liner; whereas part (b) is a photograph of the corresponding installed liner. The upstream flow perturbations due to the model at the design test condition produce the slight asymmetries in the contraction fairing as seen in figure 12(a). Figure 12(b) is a downstream view into the liner contraction with one block missing. The 14.5-in-tall office trash can establishes a relative scale for the figure. The circular cross section at the 24-ft station in

figure 12(a) is the first prominent circle outside of the white painted liner blocks seen in figure 12(b).

The swept-wing model (23° sweep) is offset from the tunnel centerline by about 12.75-in. Projections of its leading and trailing edges onto the tunnel centerline fall at the 42-ft and near the 49-ft tunnel stations, respectively. The distorted liner cross-sectional shapes in the test section, shown in figure 13, are seen to be near and downstream of the model. The double lines at the 47- and 49-ft tunnel stations in figure 13(a) show the local extent and magnitude of the displacement correction. Several "two-wall" choke contour heights are shown on the liner section at the 55.2-ft tunnel station.

Figure 13(b) is a photograph made looking upstream through the liner test section. The swept box beam, on which the LFC wing panels are to be mounted, has been installed and is seen to span the tunnel from ceiling to floor at the left of the photograph. The wing upper surface faces into the channel on the right side of the beam. The chokes appear as the large dark areas on each of the sidewalls in the foreground. In this photograph, taken in mid-December 1981, the three streamwise rows of pressure taps and the spanwise plenum vents were taped off while the liner was being installed and finished. The vertical steps in the floor and ceiling end plates are also seen in the foreground of the photograph. The two windows, seen on the right sidewall just upstream of the choke leading edge, are at the upstream end of the original 8-ft TPT test section. These windows are used to accommodate lighting and television cameras so that the model can be viewed during tunnel runs.

Figure 14 shows upstream views through the liner diffuser. Both top and bottom edges of the end-plate steps have been gradually rounded out; the fairing starts very near the model trailing edge, as seen in figure 14(a). Figure 14(b) is another upstream photograph through the liner, but it was taken from the opposite side of the tunnel and farther downstream than that of figure 13(b). The tunnel access door is at the left side of figure 14(b), and the liner was faired to accommodate it. The narrow liner blocks, seen on both sides of the bottom end-plate block which contains the step, can be removed and resized to allow for step alignment with the model trailing edge when flap or angle-of-attack changes are made. This photograph also indicates the liner-installation progress at mid-December 1981.

Figure 15 shows some details of a remotely controlled, variable-height, tunnel-sidewall choke plate. It was designed so that a choke plate on both tunnel sidewalls could be adjusted in height to choke the flow for tunnel Mach numbers between 0.8 and 0.84. Figure 15(a) is a cross-sectional schematic showing the electric motor-actuated bell-crank mechanism for remotely varying the height of the fiberglass choke plate. The piston operates through one of the original tunnel test-section window ports. The spanwise strip of porous material located just downstream of the minimum tunnel area (maximum choke height) vents the tunnel plenum and volume behind the liner. A low plenum pressure is established when the tunnel flow is choked with the shock wave standing downstream of the porous vent strips. Figure 15(b) is a close-up view of the sidewall choke plate (looking upstream) taken in March 1982. In it, the 6-in-wide, porous plenum vent strip is clearly visible.

Suction Requirements

Suction requirements under the turbulent boundary layers on both liner end plates near the model and on the model surfaces near the liner were determined as part of the liner-design procedure. This was done in the process of determining the effective displacement correction which had to be accounted for in the liner shape. Determination of the suction requirements in these turbulent-flow regions is not to be confused with what is required to determine the laminar-flow-region suction rates over most of the model. (See, e.g., refs. 1 and 27.) In addition, sizing the porosity of the plenum vent strips (see fig. 15) was based on achieving a reasonable tunnel startup time of about 10 min.

The boundaries of the wedge-shaped regions of turbulent boundary-layer flow on the LFC model surfaces were determined by assuming that the liner-end-plate turbulent boundary layer trips the model flow. The disturbance was taken to propagate at a 10° angle from the local streamline direction (ref. 28); the resulting curve was defined as the inboard boundary of the turbulent-wedge region. For the model lower surface, these boundaries are shown as dashed lines in figure 16. Increased suction levels were required over the shaded portions in order to keep the turbulent boundary layer attached throughout the adverse pressure-gradient regions on the model surface at the design test-point flow conditions. Figure 17(a) shows the calculated local magnification (CQM) of the laminar-region suction-rate levels required in the turbulent-wedge regions. Provision for even more capability was allowed for in the hardware; figure 17(b) shows the local magnification of the laminar suction rate available in the turbulent-wedge regions for off-design control. However, volume limitations in the aft region of the model would not allow for a very uniform magnification of the suction distribution. Bulkheads within the model LFC ducting system approximately follow the turbulent-wedge boundaries so that a proper accounting can be made for the suction-power contribution to the LFC drag. Even though the design-point calculations indicated no need for increased suction in the turbulent-wedge regions on the model upper

surface, some suction was also incorporated in order to allow for off-design control in the aft region where shocks would tend to occur.

Suction is required on the liner end plates near the model juncture in order to keep the turbulent boundary layer attached through the adverse pressure-gradient regions which occur as follows: on approaching the model leading edge, through the aft-portion pressure-recovery regions, and near the concave corners on the lower surface. Figure 18(a) is a schematic of the C_q levels at the design condition according to the 2-D streamline boundary-layer calculations. As can be seen, the suction is required within only 5 in. or so of both model surfaces. The liner blocks in these regions form a collar about the model containing suction panel blocks with slot/plenum/duct construction very similar to that used on the wing. These blocks are metal, but with molded fiberglass outer skin; they move with the model through angle-of-attack adjustments. The location of these suction panel blocks in the liner end plates around the model is shown in figure 18(b). It is seen that an end-plate suction panel block "above" the flap upper surface has not been included in the hardware. It was deemed to be too complex since it would have to move independently of the others with every flap adjustment. Foam shim liner blocks will be used to fair the liner between the movable collar blocks and the fixed liner blocks. Alignment of the liner steps with the model trailing edge will also be accomplished by using shim liner blocks.

Liner Instrumentation

Assessment of the aerodynamic performance of the contoured liner will be made primarily by using static-pressure measurements not only on the model but also on the liner itself. The design-point liner pressures have been generated in this design procedure and have been used as a guide in the location of pressure taps.

A number of considerations, generally related to the sensitivity of the transonic flow, lead to a requirement for many pressure measurements: for example, the lack of conventional tunnel symmetry, the small ratio of tunnel height to model chord, and the supercritical-flow conditions within the nonporous stream tube defined by the liner. From an operational point of view, one will need many measurements as a guide in "trimming" the liner locally to reach the design point (an adaptive wall) or approach an off-design point (a partially adapted wall). In fact, most of the emerging wall-interference assessment/correction procedures (see ref. 29 for a brief summary) also require pressure measurements near or at the wall as input in order to correct the model data.

About 1000 liner pressure taps have been installed, and a schematic depicting the local density on two of the walls is shown in figure 19(a). As indicated, these taps lie along streamline filaments and are approximately aligned across the tunnel at both constant sweep and constant tunnel stations. Several rows can be seen in the test-section photograph (fig. 13(b)). Data from these taps should aid in assessing the extent of yawed-wing flow at the design point and in locating the blockage problems at off-design points. According to the liner calculations, the design-point free-stream pressure is obtained ahead of the model over a short streamwise distance only on those streamlines lying on the sidewall "above" the wing upper surface, that is, the east wall in figure 19(a). Figure 19(b) shows a plot of the calculated design-point pressure-coefficient distribution along the tunnel at the "middle" of this wall. The pressure-coefficient plateau around the 36-ft tunnel station will be taken as the free-stream (or tunnel reference) value, "p_∞." Tunnel reference gages will sense the static-pressure values from taps on all three streamline filaments in this region; only one is indicated in figure 19(b).

Finished Liner

Installation of the 8-ft TPT liner and LFC swept-wing model was completed by late March 1982, and then preliminary shakedown runs of the facility began. Figure 20 presents photographs of the finished liner taken in late March and April 1982 before any LFC model testing had been done. Much of the contouring detail is not readily seen, however, because of the nearly uniform color and texture of the finished liner. The LFC model is in place; and with the protective tape covering removed, one can see how the liner blends into it. Figure 20(a) is a downstream view through the liner-contraction section. In it one can see how much the wing mean plane is offset from the tunnel centerline and also the development of the liner step resulting from the differential spanwise flow displacement in the tunnel channels "above" and "below" the wing surfaces. Figures 20(b) and (c) are downstream views through each of these two channels at the test section. The suction panel blocks are the dark areas at the top and bottom liner end plates. Figure 20(d), an upstream view through the liner diffuser section, was made just before the final finish coat was applied. Thus, more of the contouring detail can be distinguished in it.

Concluding Remarks

An overview has been presented of the entire procedure developed for the aerodynamic design of the contoured wind-tunnel liner for the NASA supercritical, laminar-flow-control (LFC), swept-wing experiment. This overview has indicated the design strategy, the sequence of steps followed, and the overall data flow. The engineering design and fabrication of parts for the liner

have been completed, and the liner is presently installed in the Langley 8-Foot Transonic Pressure Tunnel. LFC model testing has begun and preliminary test results indicate that the liner is performing as intended. Examples of the liner-design results and hardware implementation of it are given herein.

The liner designed by using this procedure is for a given swept airfoil configuration at a fixed design-point condition. The liner is also being used at off-design conditions in the LFC experiment. At subcritical conditions the liner establishes reasonably good infinite-span yawed-wing flow simulation. It should be noted that the procedure itself has a general utility which is currently restricted by limitations in calculating the viscous flow field about arbitrary configurations. The procedure is directly applicable to the two-dimensional streamlined-tunnel problem.

Langley Research Center
National Aeronautics and Space Administration
Hampton, VA 23665
July 19, 1984

Appendix A

Summary of Tasks and Computer Codes for Liner-Design Procedure

An identification of the tasks involved and computer codes used in the aerodynamic liner-design procedure is presented in this appendix. Since most of these tasks have already been addressed in the main text (see the section entitled "Liner-Design Procedure"), here we simply delineate and identify all tasks and computer codes within each of the major areas shown as the dashed-line boxes in figure 2. Our intention here is to provide for an easy association of a specific design task with a computer code and its documentation. Some of this documentation is now available, and some will be published subsequently. An outline of the data flow within and between these major areas and specific tasks is given in appendix B.

In figures A1 to A4, the specific tasks within each of the four major areas of the liner-design procedure are listed. (See fig. 2 of the main text and fig. B1 in appendix B.) At the right-hand side, the name of a computer code is associated with each task. Each task and code are described in the following discussion in the order listed in the figures. Many of the codes are basically data-processing codes geared to specific details of the present design procedure and configuration.

Test-Section Shape

The following code names refer to those shown in figure A1:

NYUFAST The NYUFAST code is the 2-D transonic analysis code (Program H) developed at NYU, as described in reference 17. It was used extensively in the LFC airfoil design work discussed in references 7 to 9. Airfoil coordinates for input to the liner design are taken from the output of this code. In the trailing-edge region, these coordinates contain a small turbulent boundary-layer displacement correction that is assumed to start at the chordwise station where the LFC suction ends in the laminar test regions on the wing.

TRANDES The TRANDES code is the transonic airfoil analysis or design code described in reference 18. It is used here in the analysis mode as the first step of the liner-design procedure since it generates a full-potential equation solution on a Cartesian grid as indicated in figure 3(a). Modifications have been made to record the flow conditions, airfoil coordinates, and surface velocities as well as the computational grid and velocity components on it. (See the main text for further comments on its use.)

STRMLYW The STRMLYW code determines inviscid, free-air, yawed-wing streamline (space) curves by integration downstream in the 3-D velocity field (u, v, w); that is, the airfoil (u, v) field plus constant sweep component (w). Initial values are an array of y-values, $y(JI)$, in a far upstream plane ($z = 0$). Thus, JI is the streamline-curve index. The integration is carried out along the wing leading-edge normal grid, $x_\perp(I)$, as depicted in figure 3(b). Thus, the generated streamline coordinates (x, y, z) are functions of the two parameters I and JI. Data files are made containing these arrays as well as arrays for pressure coefficient C_p, streamline distance s, and displacement correction Δ^* (with $\Delta^* = 0$ here). This is the basic block of streamline data processed by most of the other codes.

ASYSLTB The ASYSLTB code assembles the streamline curves generated by STRMLYW into either a top- or bottom-liner end plate (ceiling or floor, respectively). These curves are translated along the wing span according to sweep theory. The end-plate shapes contain the corner fillets and must be constrained to lie within the existing tunnel walls.

ASYSLS The ASYSLS code creates the two liner sidewalls (sides facing the upper- and lower-wing surfaces) by translating the first and last streamline curves on both end plates uniformly along the wing-span direction according to sweep theory. The assembled data arrays for both sidewalls are stored on one file. The assembled streamline curves for all walls of the test section are depicted in figure 3(c).

ENDWALY The ENDWALY code is basically a streamline-filament (space curve) data-processing code. It interpolates the curve data onto a Cartesian tunnel grid and plots various views of the liner shape, sonic lines (as shown in fig. 4, for example), and pressure-coefficient distributions. It contains provisions for calculating the liner cross-sectional areas and making Mach charts. This code also prepares the data files used to create the control tapes for the numerical milling machine. This code operates on streamline-curve data files at several places in the overall procedure.

Contraction Shape

The following codes names refer to those shown in figure A2:

GESTC The GESTC code is the General Electric stream-tube curvature (STC) code described in references 20 and 21. It is capable of analyzing transonic flow inside of either 2-D or axisymmetric ducts of variable cross-sectional area. GESTC was used first in a cut-and-try manner to obtain the axisymmetric, inviscid short-nozzle solution (shown in fig. 5(a)) upon which the liner-contraction design was based. Later in the procedure, it was used to analyze the axisymmetric equivalent of contraction fairing shapes for both inviscid and viscous calculations. This code was also extensively used in the choke-shape design; both 2-D and axisymmetric analysis modes were employed. (See ref. 26.) Code modifications were made to create data files and plot the computational grid, flow-velocity components, and other flow parameters.

UCARTN The UCARTN code interpolates the axisymmetric nozzle solution from GESTC onto a cylindrical grid. The flow solution from GESTC is on a streamline grid; interpolation of both coordinates and velocity components is done by using spline-fit routines.

UVELN The UVELN code superimposes wing-perturbation and nozzle-velocity components onto a Cartesian grid as depicted in figures 5(b) and 6(a). The model perturbation-velocity components are obtained from the 2-D data file (made by TRANDES) in accordance with sweep theory, whereas the nozzle velocities are from UCARTN. Interpolations are made by using spline-fit routines.

STRMLYN The STRMLYN code calculates a contraction fairing shape for each of the end plates separately and the two sidewalls together. An upstream integration in the 3-D velocity field, as depicted in figure 6(b), produces filaments which then must be faired into the existing tunnel contraction. Cubic spline-fit routines are used for this fairing. The tunnel cross-sectional area subtended by the liner end plate or sidewall at each station is also determined; cross-sectional views of the liner surface are plotted at each tunnel station. Data files are made for further analyses in axisymmetric nozzle and boundary-layer codes.

STRMPNC The STRMPNC code combines the subtended-area data files from STRMLYN runs for a top end plate, bottom end plate, and sidewalls in order to obtain the radius distribution of an equivalent axisymmetric nozzle. These data are used as input for both inviscid and viscous analyses in GESTC.

GESTC Discussed previously.

MRGSTRF The MRGSTRF code merges streamline-curve data files from the contraction and test section in order to be used for the liner-surface and model turbulent-region boundary-layer analyses. Upstream region data are at tunnel-axis normal planes; as the wing leading edge is approached, these data planes become aligned in the sweep direction (i.e., parallel to the wing leading edge). Thus, around the wing and downstream of it, the severe flow-variable gradients for all streamlines are at constant values of the streamline-curve parameter I.

ENDWALY Discussed previously.

Displacement Corrections

The following code names refer to those shown in figure A3:

DEFPSI The DEFPSI code is an extensively modified version of the boundary-layer analysis code discussed in references 22 and 23. It obtains a 2-D, finite-difference boundary-layer solution along streamline curves for the pressures specified. In flows where there is not a lot of symmetry upstream of some station, this code is used on all streamline curves, beginning in the tunnel reservoir. If the upstream symmetry allows for a reasonable upstream-region boundary-layer starting solution, then analyses in DEFPSI are initiated at an appropriate location with starting data obtained from code IT. The primary output data generated by the DEFPSI code are the mass-transfer rate and deficit stream-function distributions (see appendix C) along the liner and/or wing-surface streamline curves.

IT The IT code is essentially a current version of the code discussed in references 22 and 23. An option has been added to permit interaction of displacement corrections with the mean flow in 2-D or axisymmetric wind tunnels. In the present liner-design procedure, this code generated the upstream-region, boundary-layer starting-solution data used by DEFPSI. Streamline pressure data needed by IT was from the GESTC code solution for the equivalent axisymmetric shape of the inviscid contraction section. Some of the IT details have been given in reference 24.

CMFLUX The CMFLUX code merges the deficit stream-function data (see appendix C) from the liner and wing turbulent-region streamline curves. The turbulent-region deficit stream-function data for the wing are superimposed onto the local-liner streamlines by using a 1-D approximation. The total deficit stream function at a point on the liner is the sum of the local-liner value and this superimposed value. The equivalent displacement correction Δ^* on the liner is the total deficit stream function divided by the local mass-flux density; it is applied in the surface normal direction defined by the local-inviscid-liner streamline-curve data. Provisions are also included to specify wall shapes for 2-D, streamlined adaptive-wall wind tunnels. The primary output data provided by this code are the displacement-corrected streamline curves or the coordinates of adapted wind-tunnel walls.

CQDIST The CQDIST code prepares suction-rate data for use in the design of the suction hardware in the turbulent-flow regions of the model. The mass-transfer rate distributions calculated for the wing turbulent region are prepared as amplification-factor distributions (CQM) expressed with respect to the laminar-flow test-region rates. Wing-surface streamline coordinates and turbulent-region boundaries are expressed in dimensional form for coordinates along the tunnel centerline and wing-sweep directions. (See fig. 16.) Plots of the suction-rate magnification factor across the span (such as in fig. 17) are also made.

NPLTCQ The NPLTCQ code is used to extract and prepare suction-rate data for use in the design of the suction hardware in the liner around the model. The liner-surface mass-transfer-rate data arrays are obtained from auxiliary-output data files made by DEFPSI and CMFLUX.

ENDWALY Discussed previously.

Diffuser/Choke Fairing

The following code names refer to those shown in figure A4:

PUNLCRX The PUNLCRX code is used to assemble data from the top and bottom end plates and the sidewalls into arrays of liner cross-sectional coordinates (y, z) at given tunnel stations x. These data files (or cards punched from them) are used in conjunction with the existing 8-ft TPT shape for a liner diffuser-section design.

WALL The WALL code generates the existing 8-ft TPT wall shape from tabular data and equations. Both cross-sectional shape and streamwise area-distribution data are generated and can be plotted.

DIF The DIF code is used to modify geometrically cross-sectional shapes in order to arrive at a liner diffuser section compatible with the liner test-section shape and the existing 8-ft TPT diffuser. It is used in a cut-and-try mode. Filleting of the liner end-plate vertical steps from the wing trailing edge to near the choke plate was done by maintaining locally the extended test-section areas of the liner. This code calculates the area and plots the shape of cross-sectional curves. The cross-sectional shape of the local-liner diffuser is interpolated between an upstream liner shape and a downstream tunnel shape so that its area matches that required from a smooth extension of the liner to the existing tunnel diffuser lines.

CMP The CMP code fits a curvature-matching polynomial to end-point data appropriate to values at the choke-plate maximum (tunnel throat) and upstream and downstream ends. A number of shapes and their influence on choked duct flow were examined in reference 26 by using the GESTC code.

GESTC Discussed previously.

CHOKE The CHOKE code is used to get the nominal choke-plate height at the throat location. It calculates the area changes due to a specified choke height for a liner cross section with corner fillets. It is iterated in a cut-and-try manner until the area change required to choke the flow is obtained.

CMP Discussed previously.

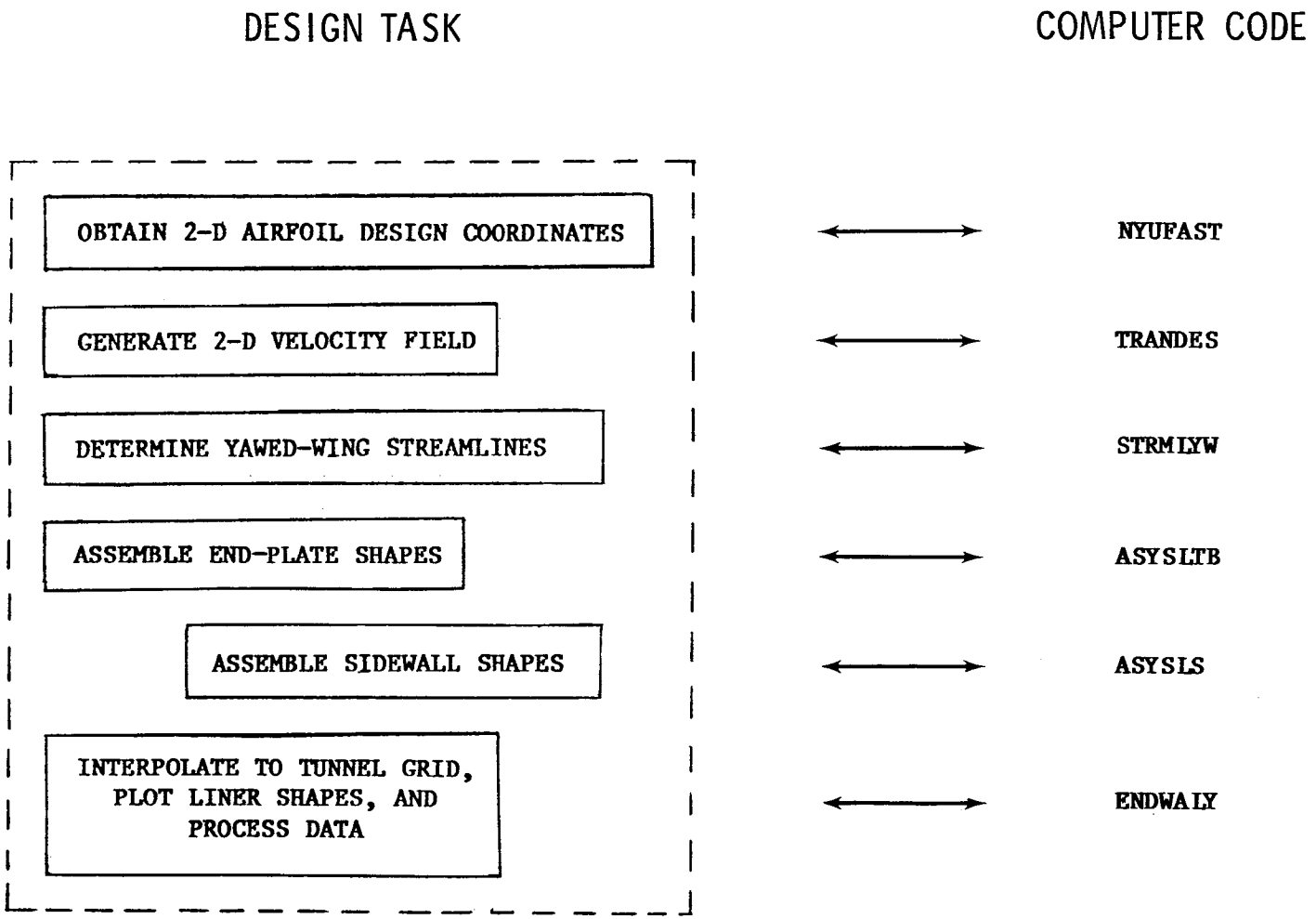

Figure A1. Tasks and codes of inviscid liner-design procedure for test section shape.

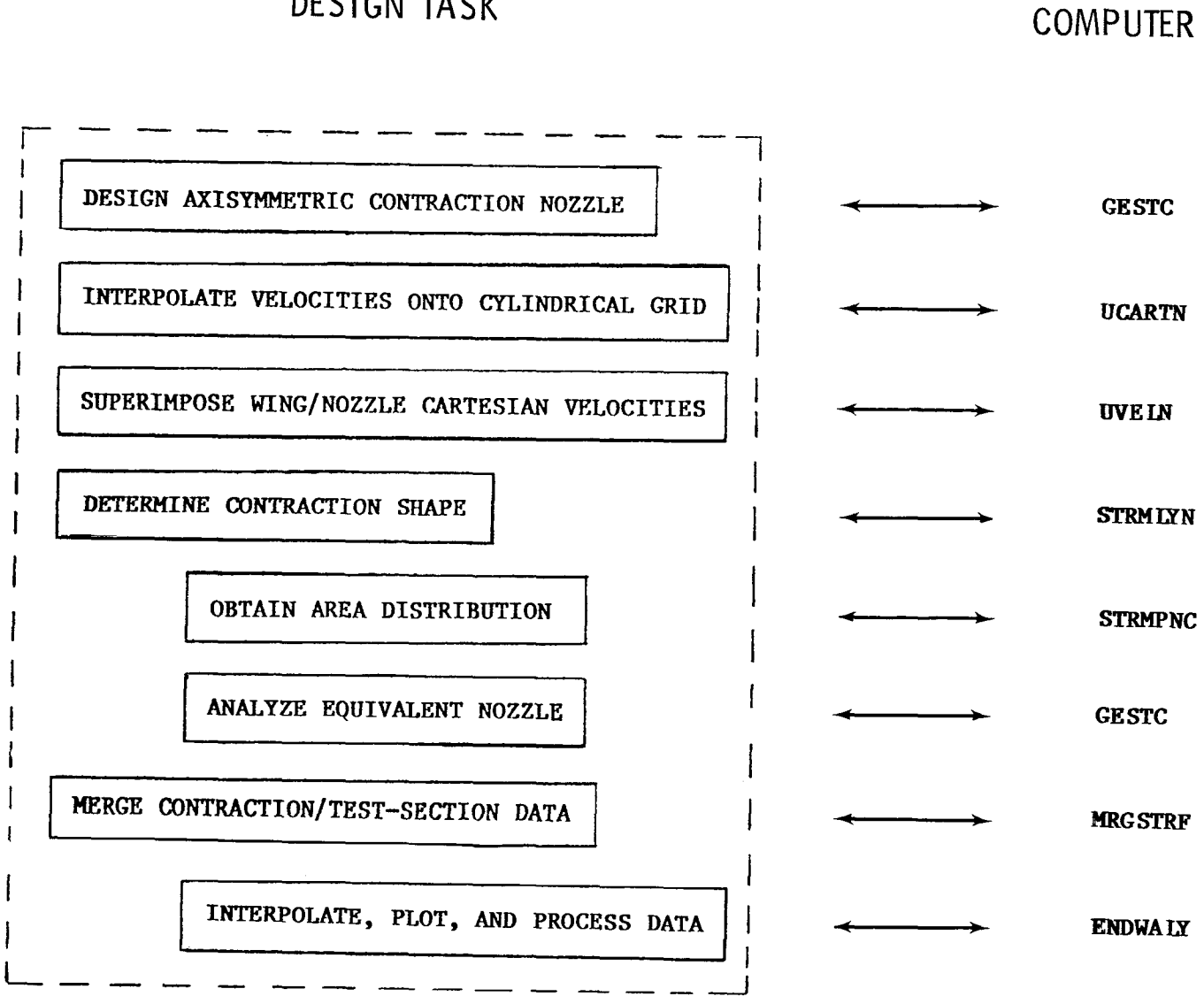

Figure A2. Tasks and codes of inviscid liner-design procedure for contraction shape.

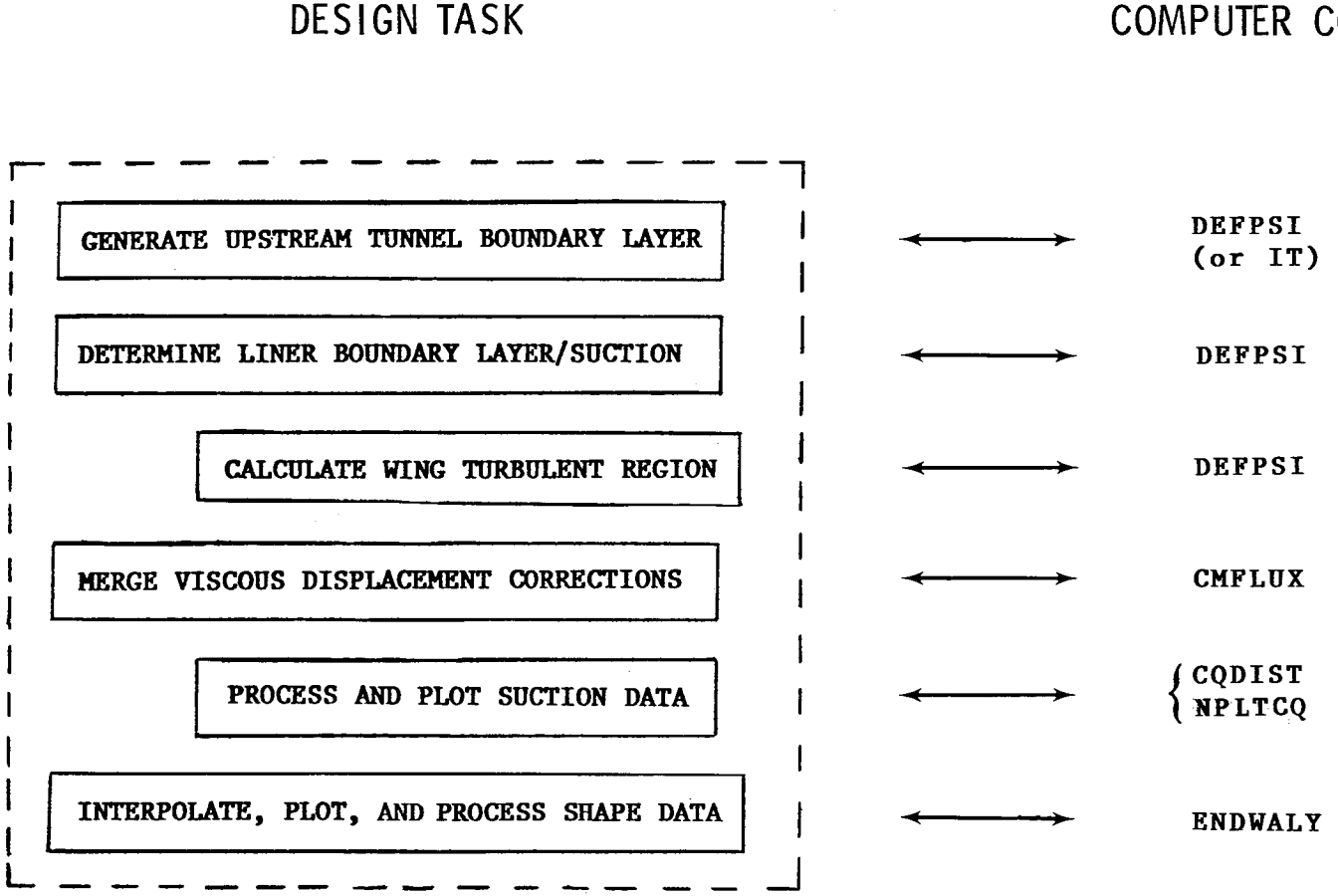

Figure A3. Tasks and codes of viscous and suction displacement-correction procedure to get final shape.

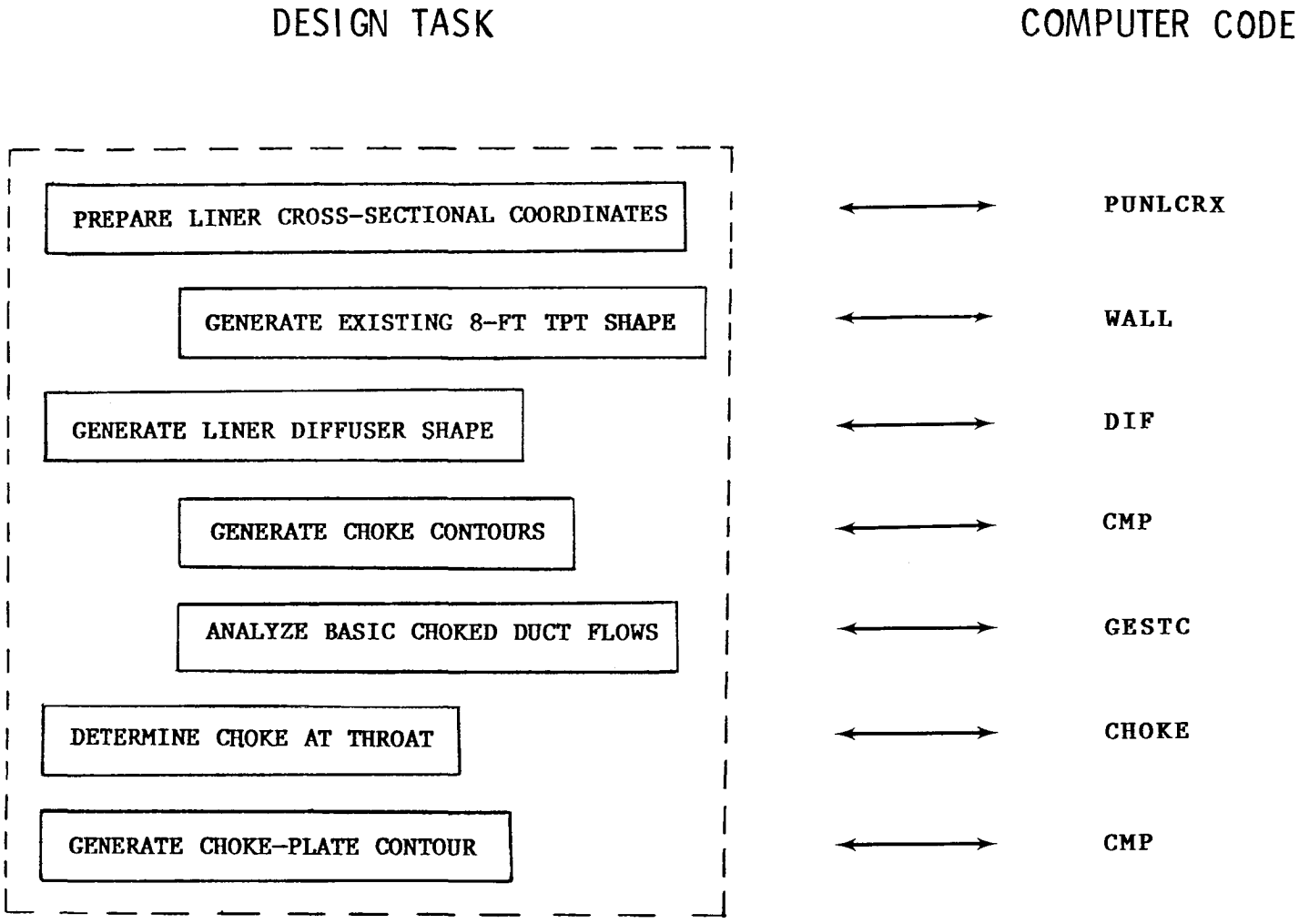

Figure A4. Tasks and codes of liner-design procedure for diffuser fairing and choke-plate shapes.

APPENDIX B

Outline of Data Flow Within Liner-Design Procedure

A chart outlining the data flow within the aerodynamic liner-design procedure is given as figure B1. The task descriptions, rather than code names, of figures A1 to A4 have been used since they are indicative of the data being passed on or the operation performed upon the data stream. Again, the dashed-line boxes correspond to the major areas shown in figure 2. In figure B1, the arrows represent transfer, generally via computer files, of data which describe the flow conditions, properties, and/or liner shape.

At several steps, there are input parameters which must be iterated in order to satisfy constraints such as those imposed by aerodynamic considerations, the existing tunnel, liner construction, model mounting, and access. Some of these iterations are within a given depicted task (code), whereas others are global; most all iterations, however, are accomplished in a cut-and-try manner. The feedback data loops for these have not been shown in figure B1. Some of the global iterations, particularly with respect to streamwise location and sizing of major components, were done before the design-procedure codes were completed. The data flow for the final liner-design iteration is depicted in figure B1. This procedure is mechanized but not automated; there is user iteraction between most of the tasks. There are a few codes which simply process the data and perhaps could be combined with other codes. It should also be noted here that figure B1 depicts the procedure and data flow which produce the aerodynamic liner-design files and data shown at the top left of figure 8.

Once the bottom end plate (BE), top end plate (TE), and liner sidewall (SW) data files have been assembled, they are generally processed independently. That is, three separate runs of the same code are required to perform a given operation on the liner data. Since it is unreasonable to indicate here descriptions of input to specific tasks (codes), we simply note that tunnel and experiment size constraints enter at the top of all the dashed-line boxes.

Two-dimensional tunnel simulations and adapted-wall calculations are accomplished by bypassing the contraction design tasks. The data files made at the inviscid test-section design for zero sweep can be directly processed through the analyses codes for viscous and suction displacement corrections. However, these data paths are not shown in figure B1.

APPENDIX B

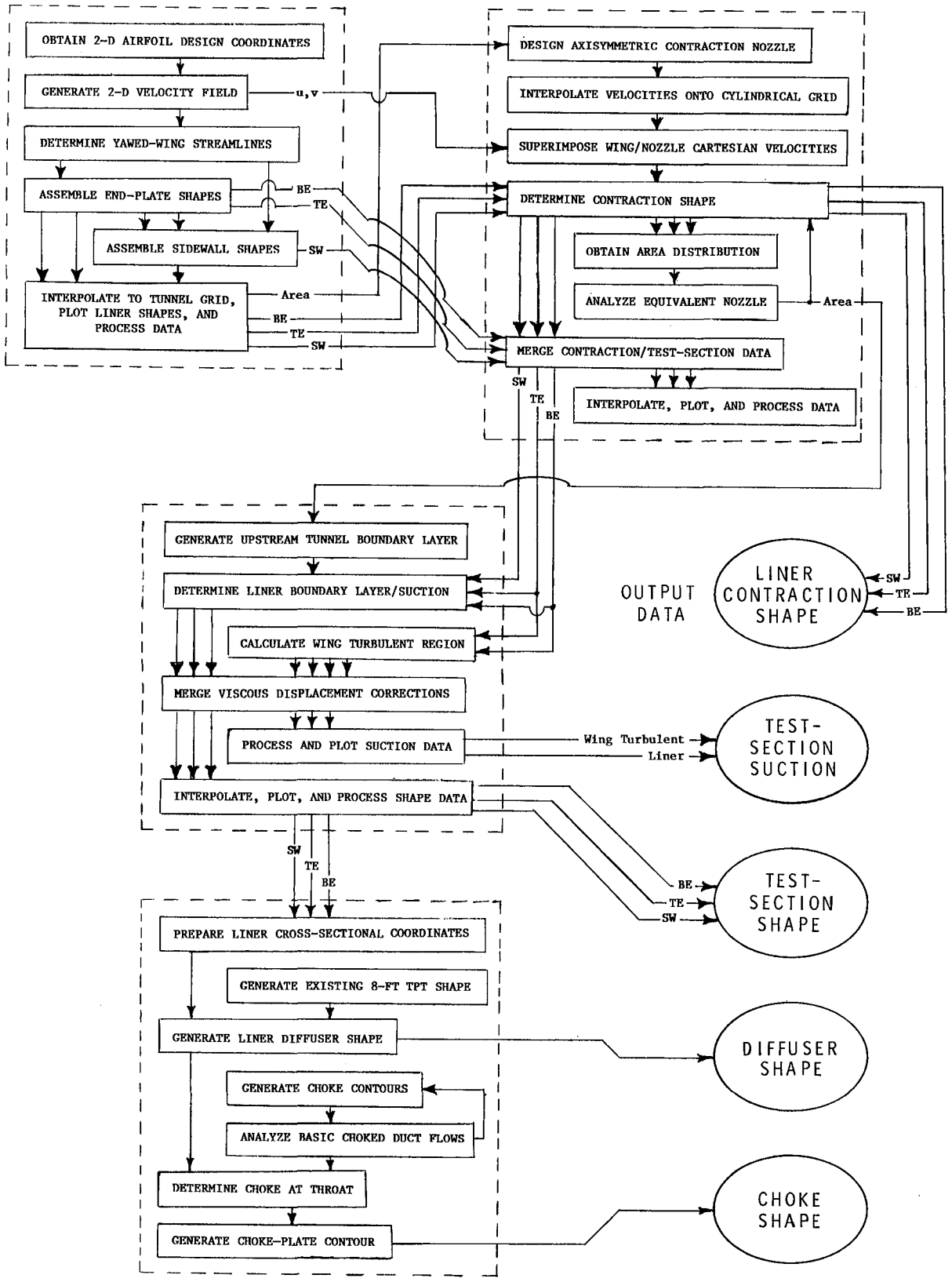

Figure B1. Details of data flow among tasks of liner-design procedure.

APPENDIX C

Deficit Stream Function for Equivalent Displacement Corrections Due to Viscous and Suction Effects

An equivalent displacement correction is required which reasonably accounts for the blockage due to viscous and suction effects on all liner and model surfaces, as well as that of the wake in the presence of the model pressure field. Model construction and original tunnel constraints require, in some places, that the local correction be applied at another place or surface. That is, a local correction at one place may need to be translated and superimposed on the local correction at another place or at several other places. In addition, it was not clear at the outset of this design effort whether the mass removal within the thick boundary layer on the tunnel-wall/liner surface should be accomplished and modeled by scoops (surface tangential flow removal) or by distributed area suction (surface normal flow removal). Finally, it was felt that it would be safer to make a correction relative to that at a given station rather than to make an absolute one.

The displacement-correction data generated by the boundary-layer codes (refs. 22 to 24) are expressed in terms of the local deficit stream function $\Delta\psi(s)$, which is defined along each streamline filament of a boundary as

$$\Delta\psi(s) = \rho_e u_e \delta^* + \int_{s_0}^{s} C_q ds - \sum_{0}^{N} \Delta\psi_n - \Delta\psi(s_0) + \Delta\psi_{tr} \tag{C1}$$

where s is the local arc length along the filament. In equation (C1), the first term on the right side corresponds to the customary boundary-layer displacement-thickness correction δ^* at the local edge conditions $\rho_e u_e$; the second term is due to the distributed surface mass flux C_q (where $C_q < 0$ for suction); the third term represents the mass loss $\Delta\psi_n$ at each of n (where $0 \leq n \leq N$) discrete boundary-layer scoops; the fourth term is the deficit stream function at $s = s_0$ and, if nonzero, makes the effective displacement correction a relative one; and the fifth term $\Delta\psi_{tr}$ represents that contribution, to be applied locally, which was translated from another place. The local equivalent displacement correction $\Delta^*(s)$, along a streamline filament of the liner, is then

$$\Delta^*(s) = \Delta\psi(s)/\rho_e u_e \tag{C2}$$

and it is applied in a direction normal to the local liner surface.

It should be pointed out that equation (C1) is also valid for mass injection; however, one must be sure that the injected mass is not accounted for twice. That is, the calculation of δ^* itself (in the first term) may already include the injected mass effects. For the case of mass removal, the present definition (eq. (C1)) of the deficit stream function is equivalent to the effective displacement-thickness definition given in reference 25. The present definition is preferred for this liner application since integration of it across streamline filaments yields the deficit mass flux. This, then, defines the one-dimensional equivalent deficit stream function which can be translated across streamlines or to another surface and be applied there at the appropriate edge conditions upon using equation (C2). For example, the correction for the turbulent-wedge regions on the LFC model are translated and applied on the liner end plate in this way. Also, some large local corrections on the liner near the model were redistributed laterally in the same way.

References

1. Harvey, W. D.; and Pride, J. D.: The NASA Langley Laminar Flow Control Airfoil Experiment. AIAA-82-0567, Mar. 1982.
2. Newman, Perry A.; and Anderson, E. Clay: Analytical Design of a Contoured Wind-Tunnel Liner for Supercritical Testing. *Advanced Technology Airfoil Research, Volume I*, NASA CP-2045, Part 2, 1979, pp. 499–509.
3. Newman, Perry A.; and Anderson, E. Clay: *Numerical Design of Streamlined Tunnel Walls for a Two-Dimensional Transonic Test.* NASA TM-78641, 1978.
4. Everhart, Joel L.: *A Method for Modifying Two-Dimensional Adaptive Wind-Tunnel Walls Including Analytical and Experimental Verification.* NASA TP-2081, 1983.
5. Newman, Perry A.; Anderson, E. Clay; and Peterson, John B., Jr.: Numerical Design of the Contoured Wind-Tunnel Liner for the NASA Swept-Wing LFC Test. AIAA-82-0568, Mar. 1982.
6. Pfenninger, W.; Gross, Lloyd; and Bacon, John W., Jr. (appendix I by G. S. Raetz): *Experiments on a 30° Swept 12%-Thick Symmetrical Laminar Suction Wing in the 5-Ft by 7-Ft Michigan Tunnel.* Rep. No. NAI-57-317 (BLC-93), Northrop Aircraft, Inc., Feb. 1957.
7. Allison, Dennis O.; and Dagenhart, John R.: Design of a Laminar-Flow-Control Supercritical Airfoil for a Swept Wing. *CTOL Transport Technology—1978*, NASA CP-2036, Part I, 1978, pp. 395–408.
8. Pfenninger, W.; Reed, Helen L.; and Dagenhart, J. R.: Design Considerations of Advanced Supercritical Low Drag Suction Airfoils. *Viscous Flow Drag Reduction*, Gary R. Hough, ed., AIAA, c.1980, pp. 249–271.
9. Allison, Dennis O.: *Inviscid Analysis of Two Supercritical Laminar-Flow-Control Airfoils at Design and Off-Design Conditions.* NASA TM-84657, 1983.
10. Harvey, William D.; Stainback, P. Calvin; and Owen, F. Kevin: *Evaluation of Flow Quality in Two Large NASA Wind Tunnels at Transonic Speeds.* NASA TP-1737, 1980.
11. Keefe, Laurence R.: *A Study of Acoustic Fluctuations in the Langley 8-Foot Transonic Pressure Tunnel.* NASA CR-158983, 1979.
12. Brooks, Joseph D.; Stainback, P. Calvin; and Brooks, Cuyler W., Jr.: Additional Flow Quality Measurements in the Langley Research Center 8-Foot Transonic Pressure Tunnel. *A Collection of Technical Papers—AIAA 11th Aerodynamic Testing Conference*, Mar. 1980, pp. 138–145. (Available as AIAA-80-0434.)
13. Harvey, W. D.; and Bobbitt, P. J.: Some Anomalies Between Wind Tunnel and Flight Transition Results. AIAA-81-1225, June 1981.
14. McKinney, Marion O.; and Scheiman, James: *Evaluation of Turbulence Reduction Devices for the Langley 8-Foot Transonic Pressure Tunnel.* NASA TM-81792, 1981.
15. Scheiman, James: *Considerations for the Installation of Honeycomb and Screens To Reduce Wind-Tunnel Turbulence.* NASA TM-81868, 1981.
16. Scheiman, James; and Brooks, J. D.: A Comparison of Experimental and Theoretical Turbulence Reduction From Screens, Honeycomb and Honeycomb-Screen Combinations. *A Collection of Technical Papers—AIAA 11th Aerodynamic Testing Conference*, Mar. 1980, pp. 129–137. (Available as AIAA-80-0433.)
17. Bauer, Frances; Garabedian, Paul; Korn, David; and Jameson, Antony: Supercritical Wing Sections II. Volume 108 of *Lecture Notes in Economics and Mathematical Systems*, Springer-Verlag, 1975.
18. Carlson, Leland A.: *TRANDES: A FORTRAN Program for Transonic Airfoil Analysis or Design.* NASA CR-2821, 1977.
19. Newman, Perry A.; and South, Jerry C., Jr.: Influence of Nonconservative Differencing on Transonic Streamline Shapes. *AIAA J.*, vol. 14, no. 8, Aug. 1976, pp. 1148–1149.
20. Keith, J. S.; Ferguson, D. R.; Merkle, C. L.; Heck, P. H.; and Lahti, D. J.: *Analytical Method for Predicting the Pressure Distribution About a Nacelle at Transonic Speeds.* NASA CR-2217, 1973.
21. Ferguson, D. R.; and Keith, J. S.: *Modifications to the Streamtube Curvature Program. Volume I—Program Modifications and User's Manual.* NASA CR-132705, 1975.
22. Anderson, E. C.; and Lewis, C. H.: *Laminar or Turbulent Boundary-Layer Flows of Perfect Gases or Reacting Gas Mixtures in Chemical Equilibrium.* NASA CR-1893, 1971.
23. Miner, E. W.; Anderson, E. C.; and Lewis, Clark H.: *A Computer Program for Two-Dimensional and Axisymmetric Nonreacting Perfect Gas and Equilibrium Chemically Reacting Laminar, Transitional and/or Turbulent Boundary Layer Flows.* VPI-E-71-8, May 1971. (Available as NASA CR-132601.)
24. Anderson, E. Clay: *User Guide for STRMLN: A Boundary-Layer Program for Contoured Wind-Tunnel Liner Design.* NASA CR-159058, 1979.
25. Fannelop, T. K.: Displacement Thickness for Boundary Layers With Surface Mass Transfer. *AIAA J.*, vol. 4, no. 6, June 1966, pp. 1142–1144.
26. Campbell, Richard L.: *Computer Analysis of Flow Perturbations Generated by Placement of Choke Bumps in a Wind Tunnel.* NASA TP-1892, 1981.
27. Dagenhart, J. Ray: *Amplified Crossflow Disturbances in the Laminar Boundary Layer on Swept Wings With Suction.* NASA TP-1902, 1981.
28. Fischer, Michael C.: Spreading of a Turbulent Disturbance. *AIAA J.*, vol. 10, no. 7, July 1972, pp. 957–959.
29. Newman, P. A.; and Kemp, W. B., Jr.: Wall-Interference Effects: Status Review and Planned Experiments in NTF. *High Reynolds Number Research—1980*, L. Wayne McKinney and Donald D. Baals, eds., NASA CP-2183, 1981, pp. 123–141.

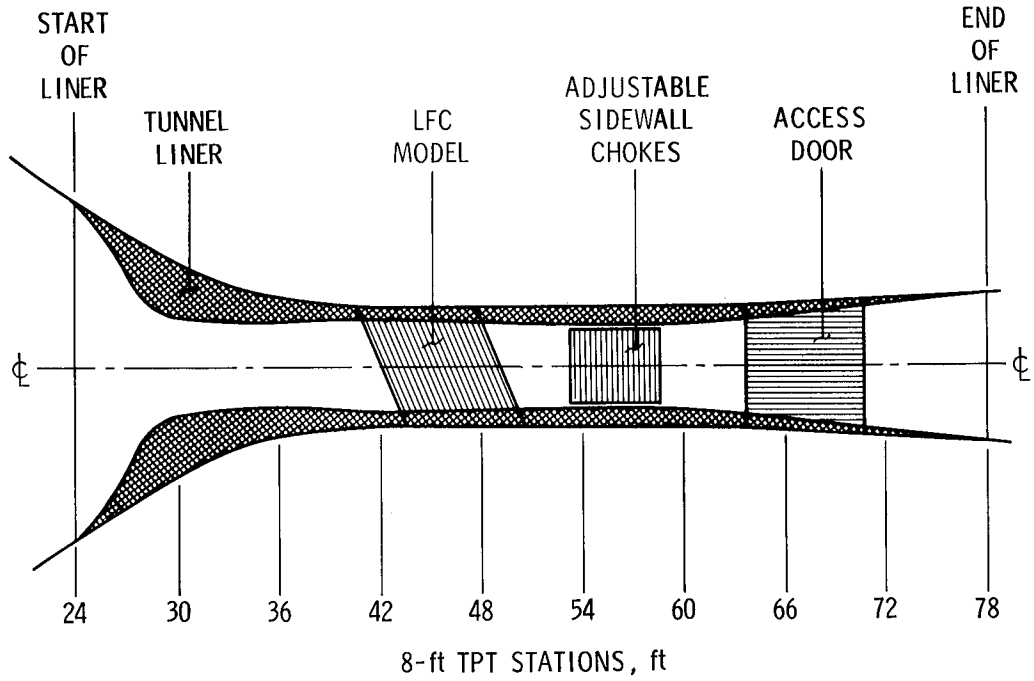

Figure 1. West side view of LFC test setup in 8-ft TPT.

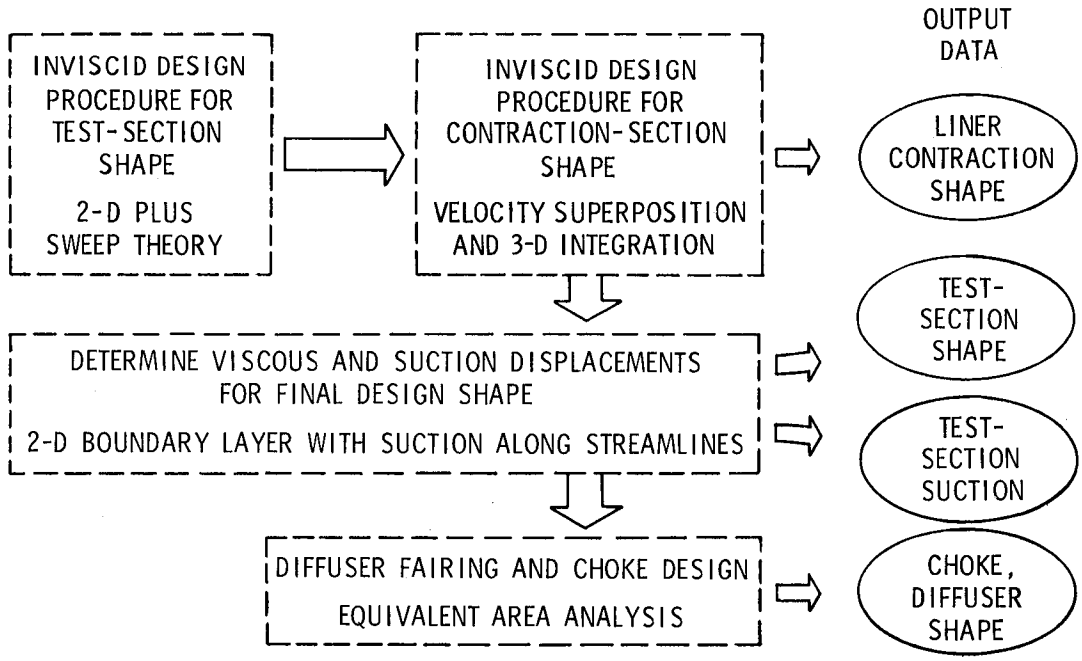

Figure 2. Outline of liner-design procedure.

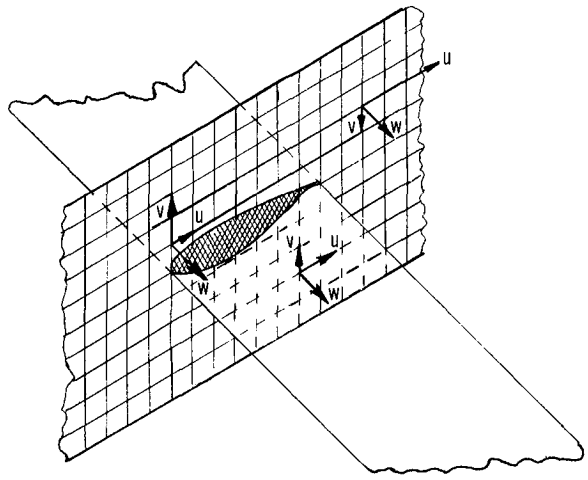

(a) Velocity field.

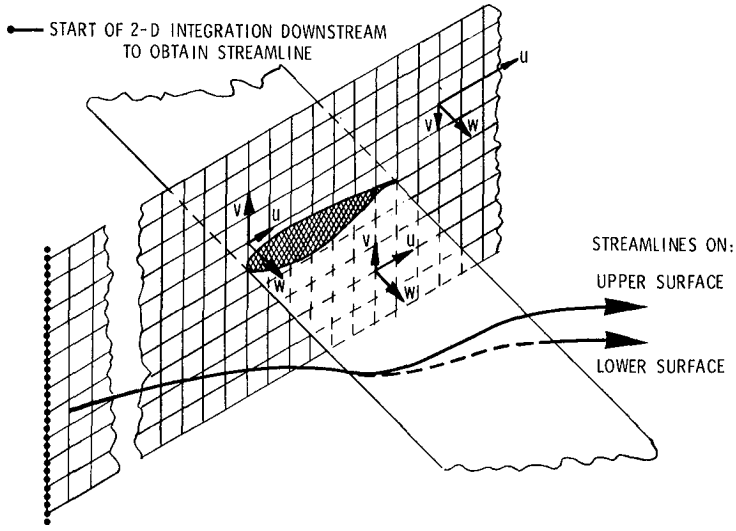

(b) Streamline filaments.

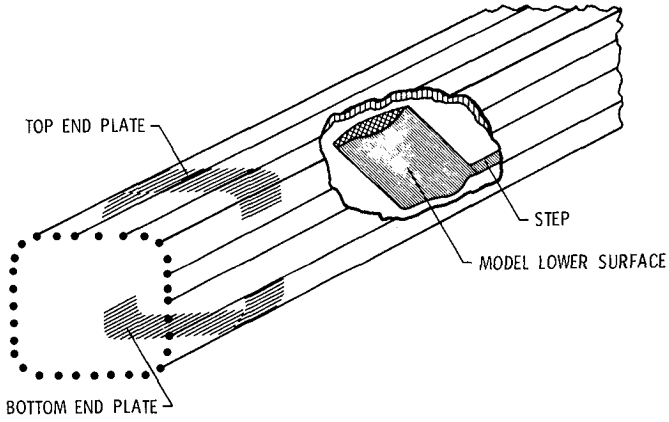

(c) Assembled streamline filaments.

Figure 3. Integration in 3-D velocity field composed of 2-D airfoil plus constant sweep components.

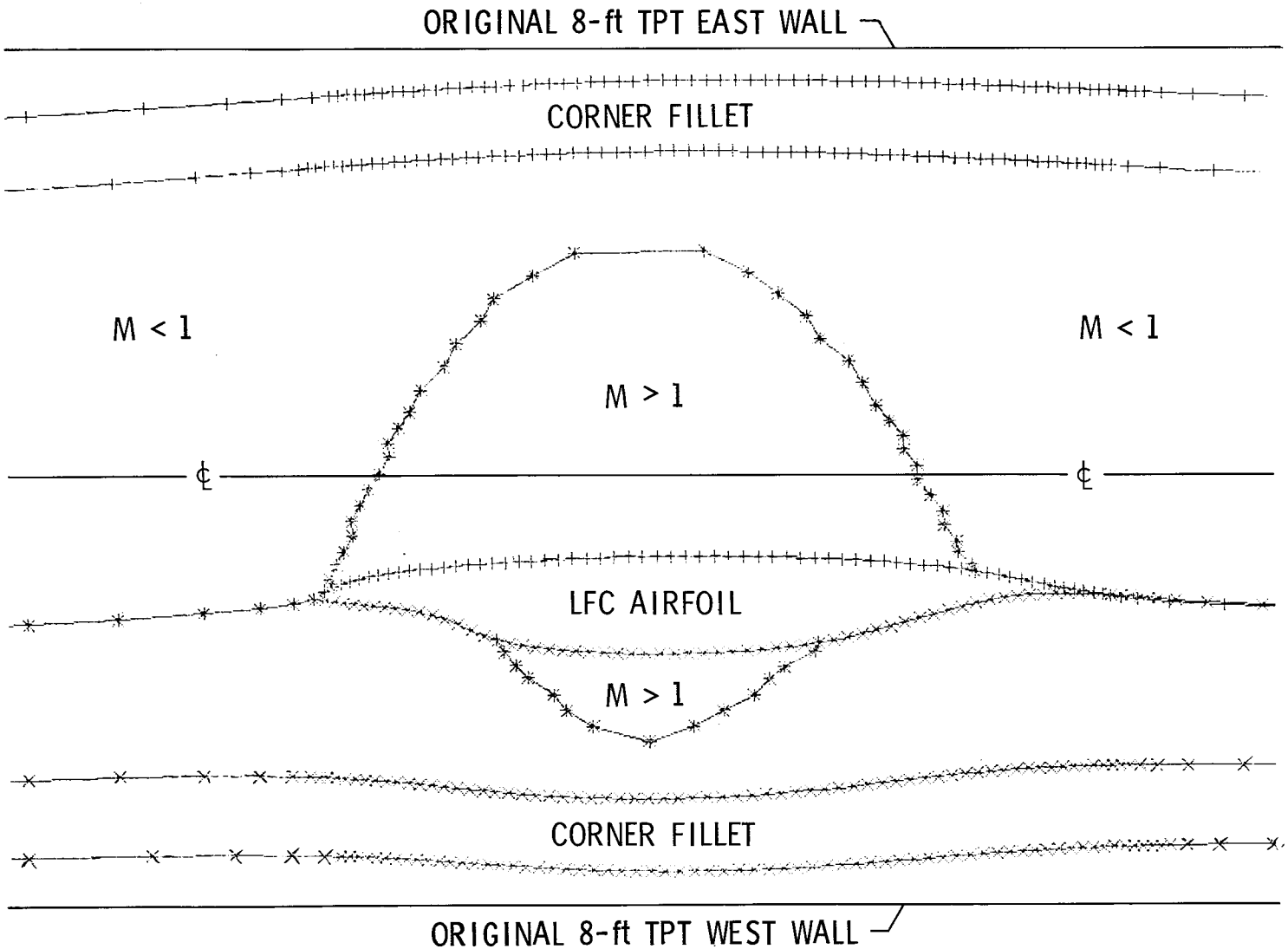

Figure 4. Top view of liner bottom end plate. Inviscid shape.

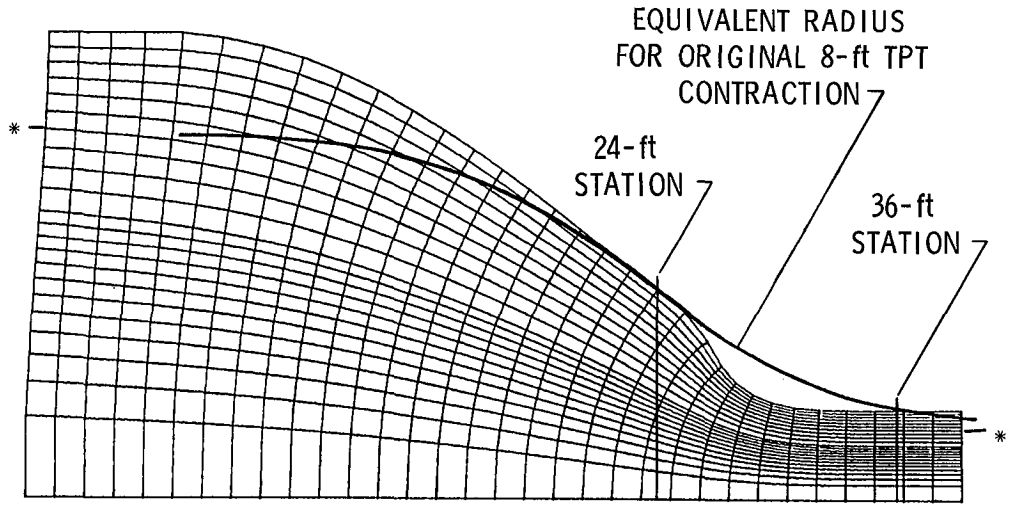

(a) Stream-tube code grid.

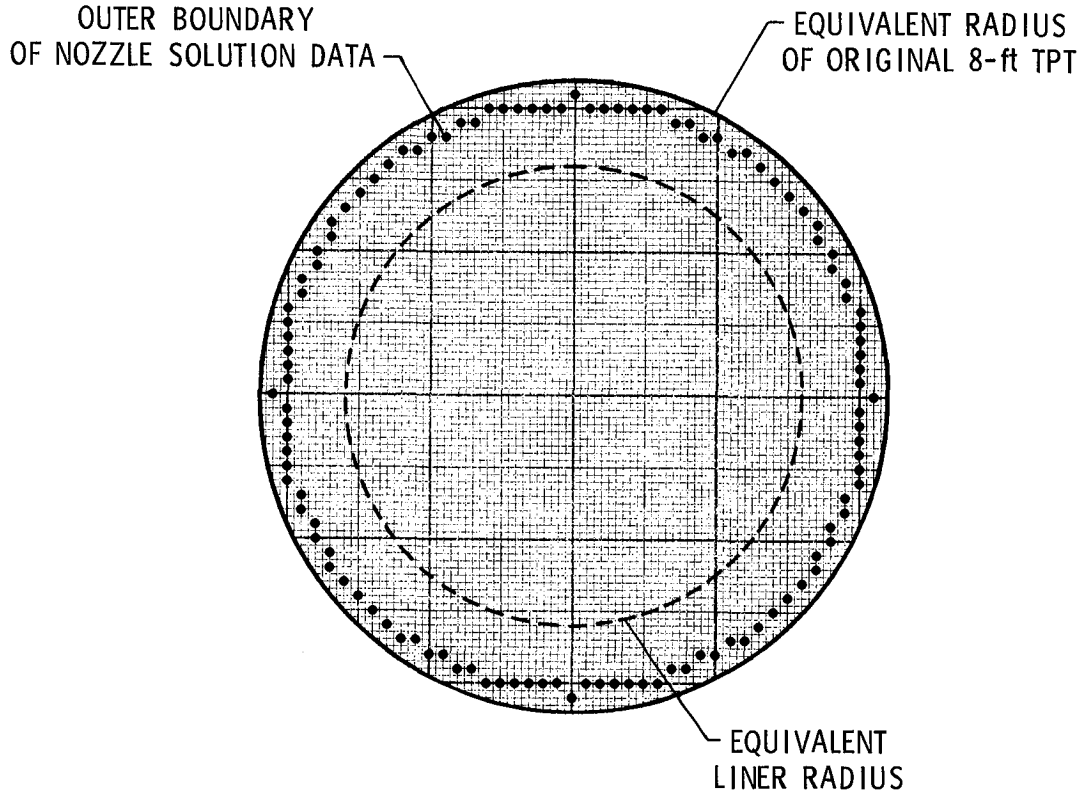

(b) Cartesian tunnel grid at 36-ft station.

Figure 5. Axisymmetric nozzle for contraction design.

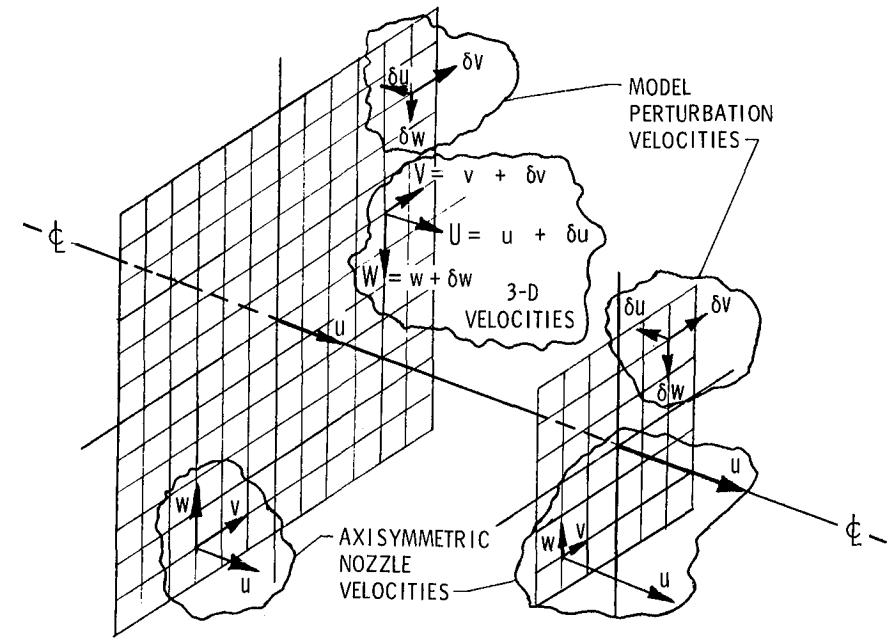

(a) Velocity field.

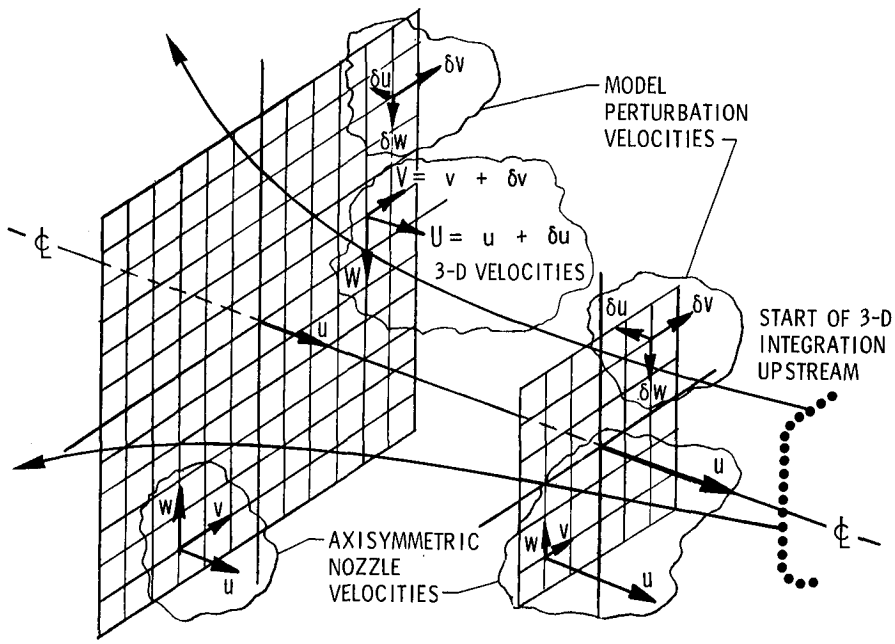

(b) Streamline filaments.

Figure 6. Integration in 3-D velocity field composed of axisymmetric nozzle plus wing perturbation components.

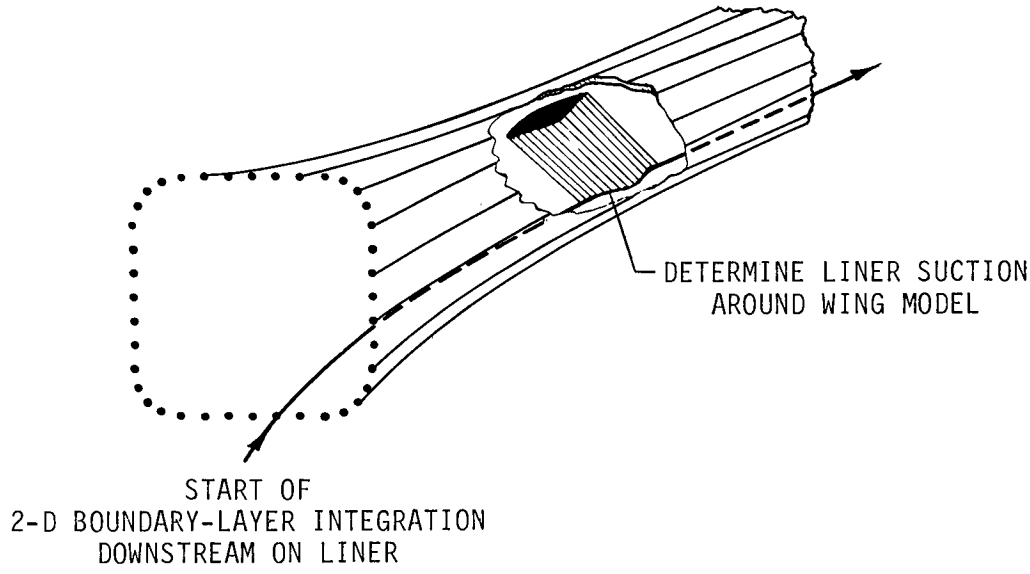

(a) Liner surface.

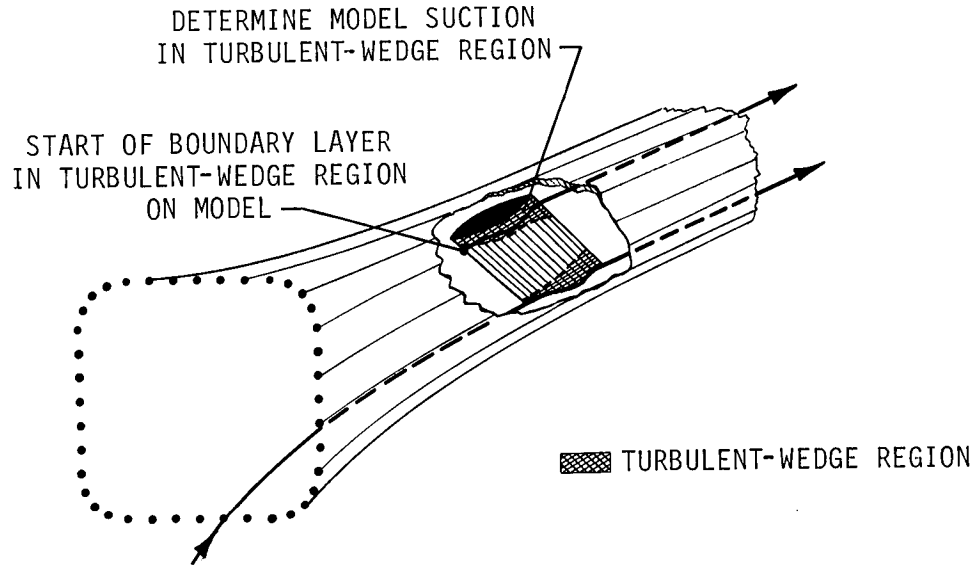

(b) Model turbulent region.

Figure 7. Integration for 2-D boundary layers on liner and model.

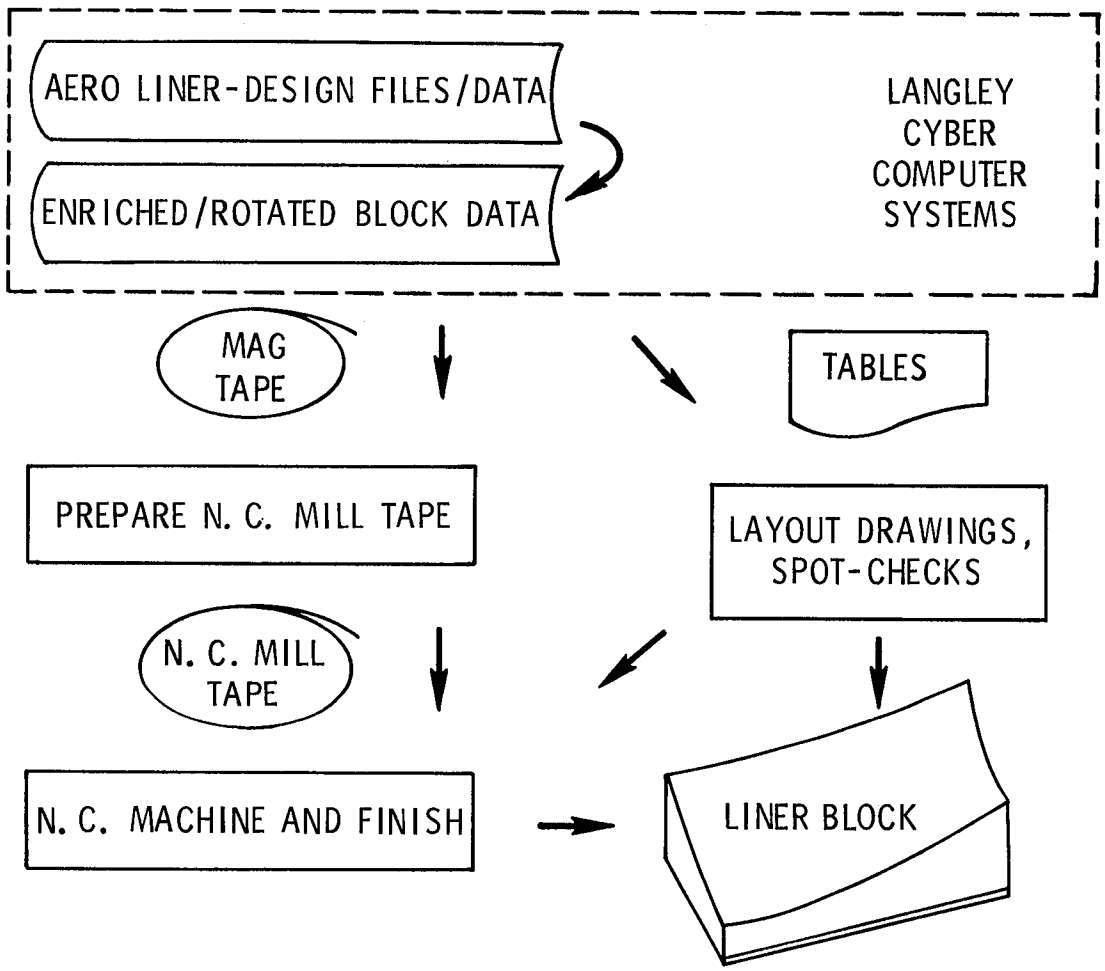

Figure 8. Final liner-shape data flow.

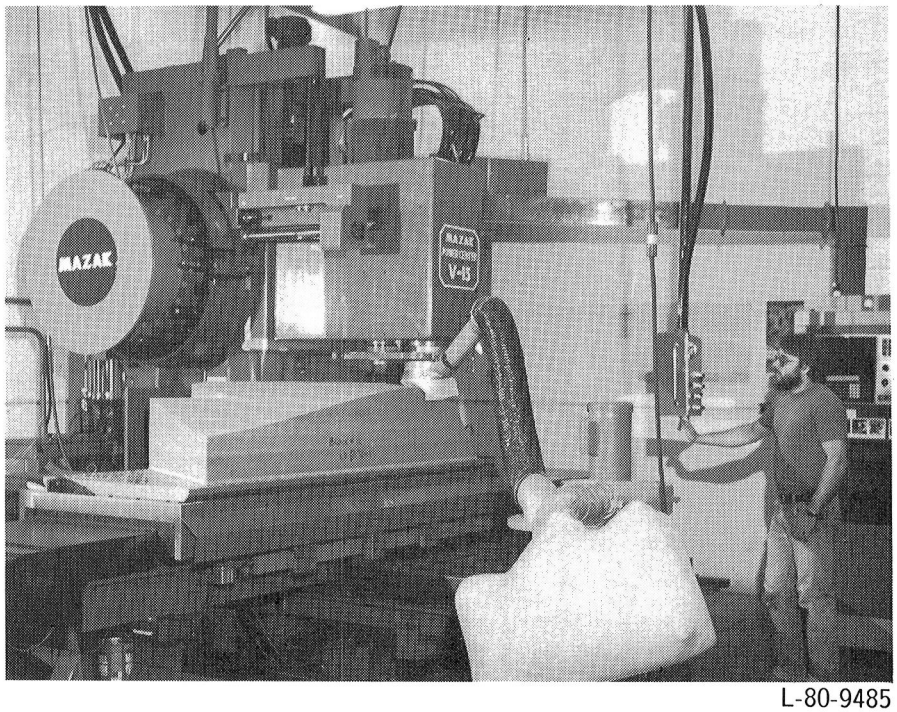

L-80-9485

(a) Numerical milling.

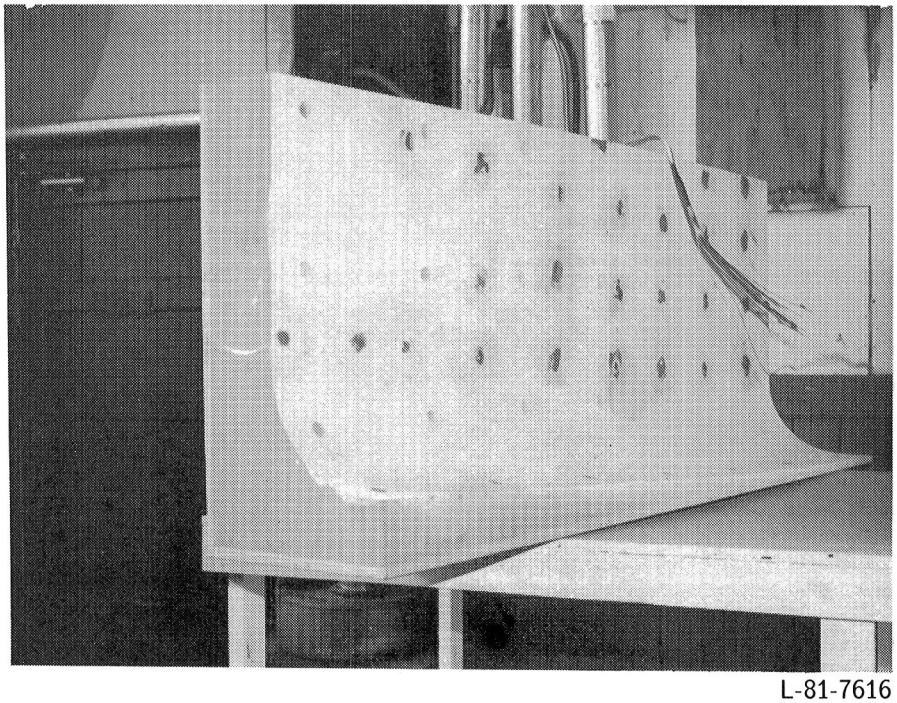

L-81-7616

(b) Sample block.

Figure 9. Liner-block fabrication.

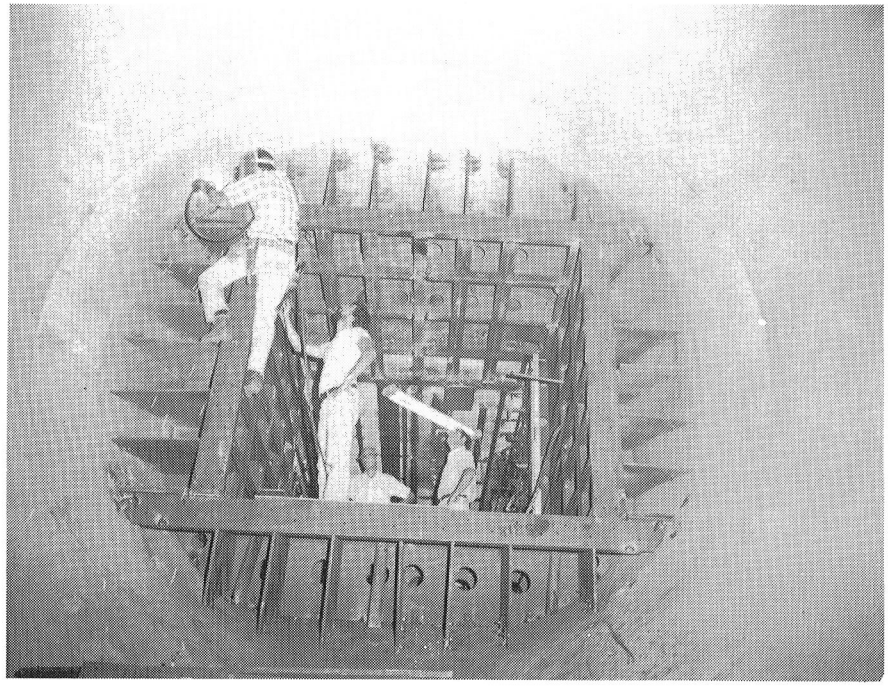

L-81-7727

(a) Support beams.

L-81-8070

(b) Ribs and one plate.

Figure 10. Liner contraction-section substructure.

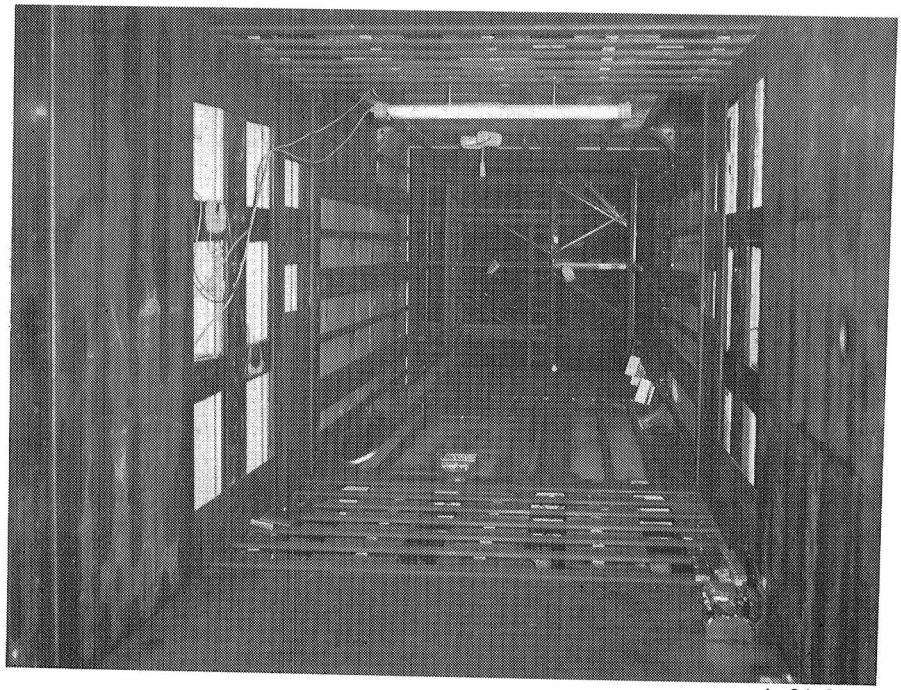

L-81-8746

(a) Upstream view.

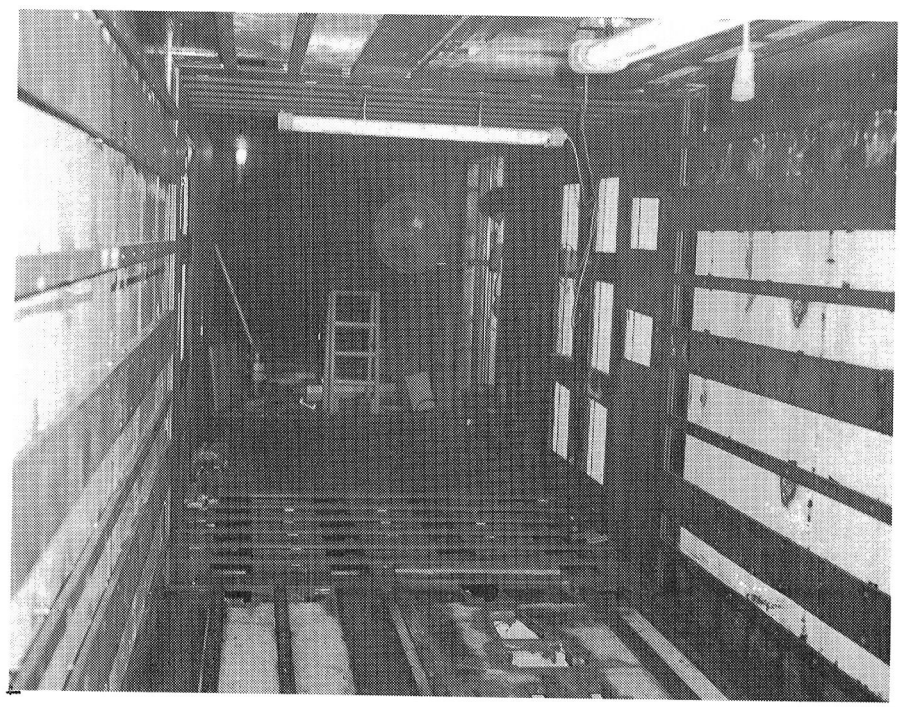

L-81-8747

(b) Downstream view.

Figure 11. Liner test-section substructure.

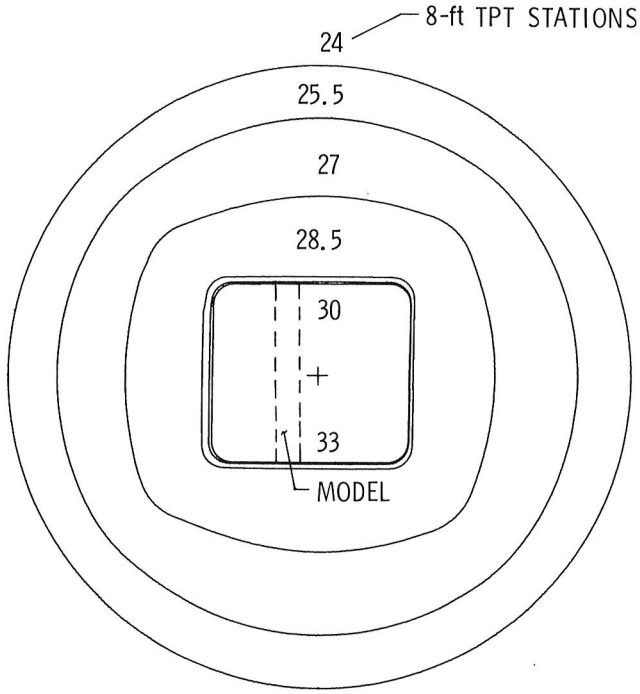

(a) Upstream cross-sectional views.

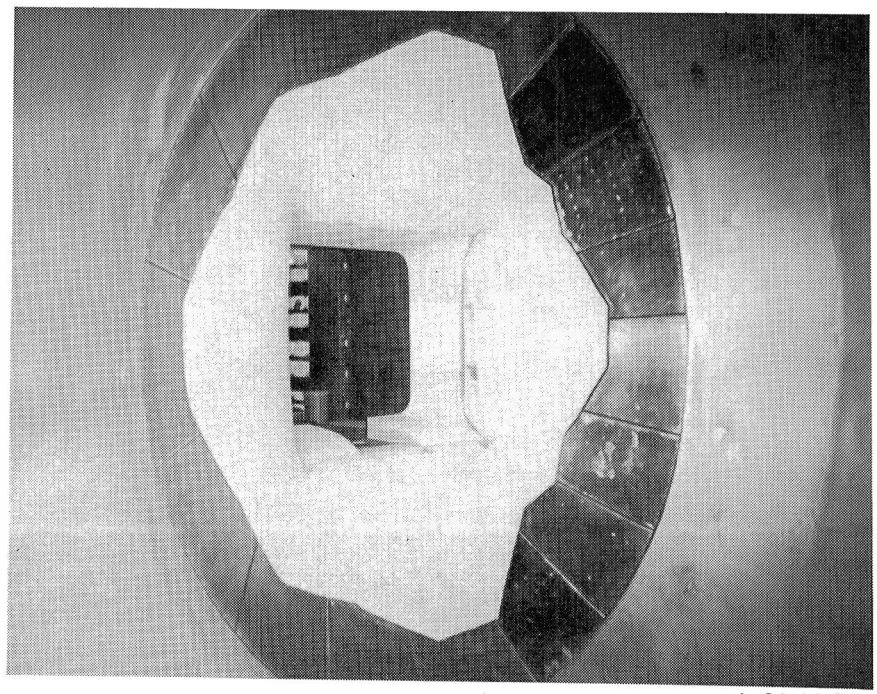

L-81-11,046

(b) Downstream view.

Figure 12. Final design shape for liner contraction section.

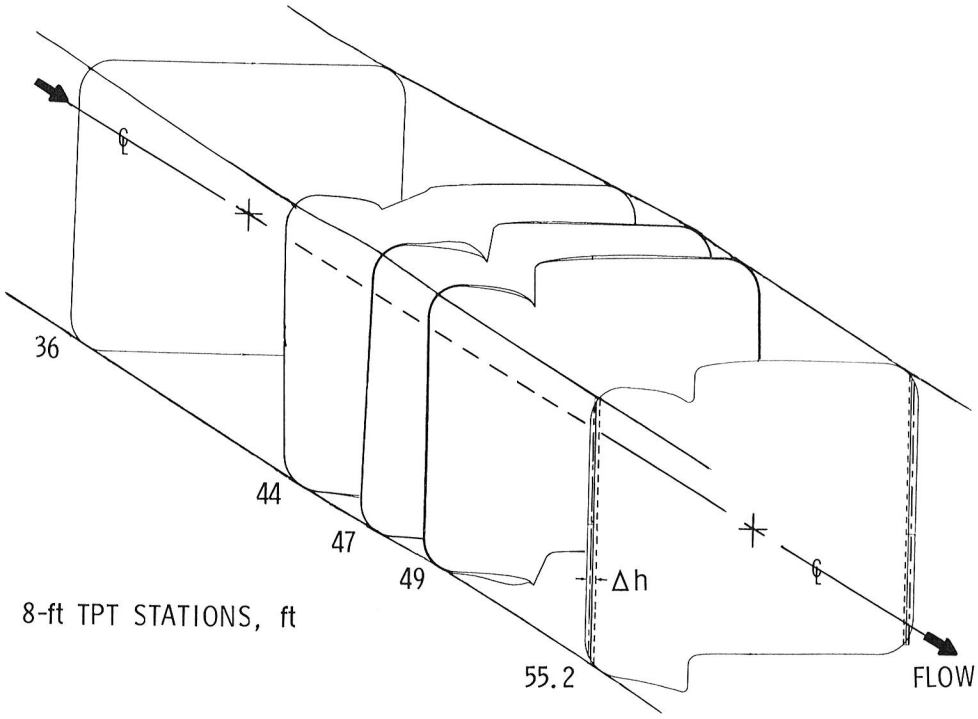

(a) Upstream cross-sectional views.

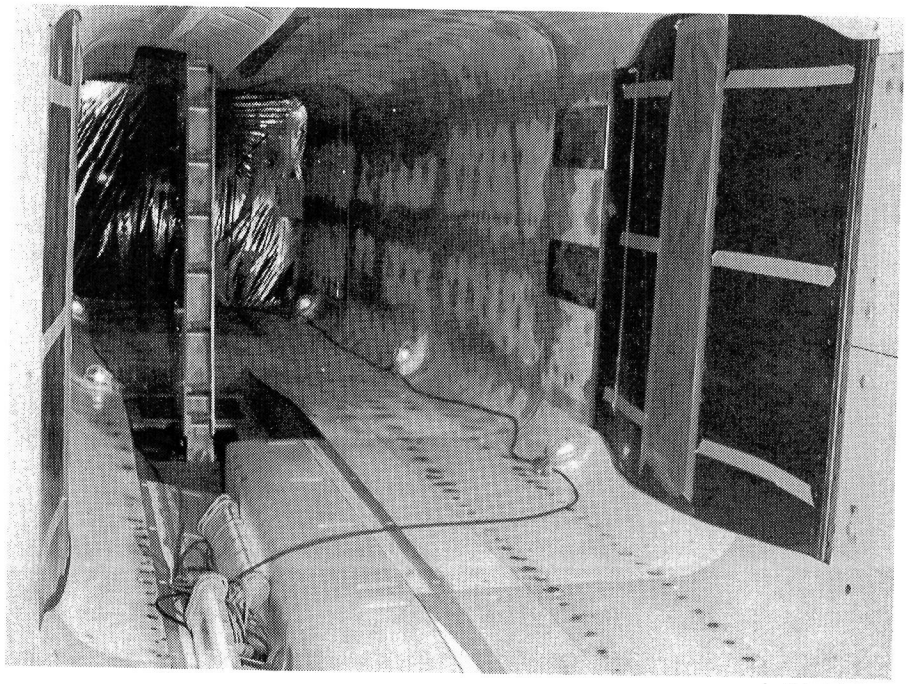

L-81-11,919

(b) Upstream view.

Figure 13. Final design shape for liner test section.

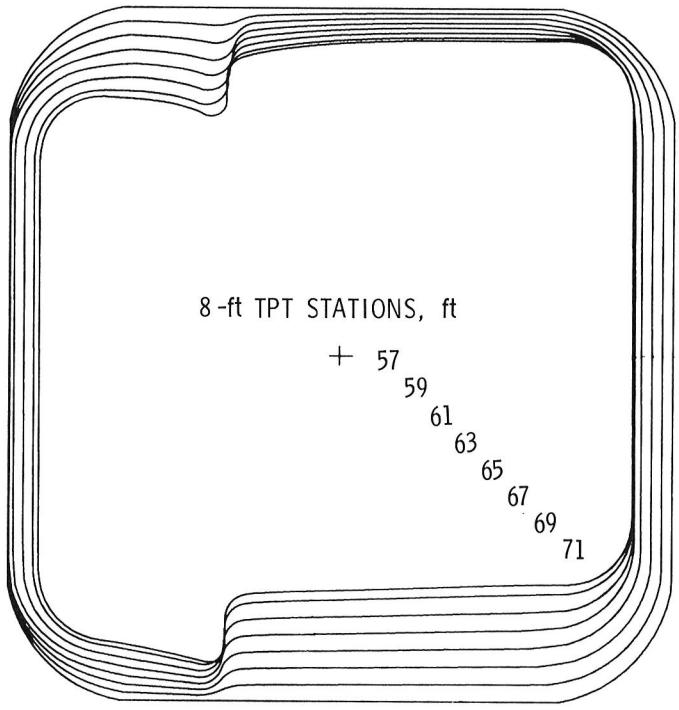

(a) Upstream cross-sectional views.

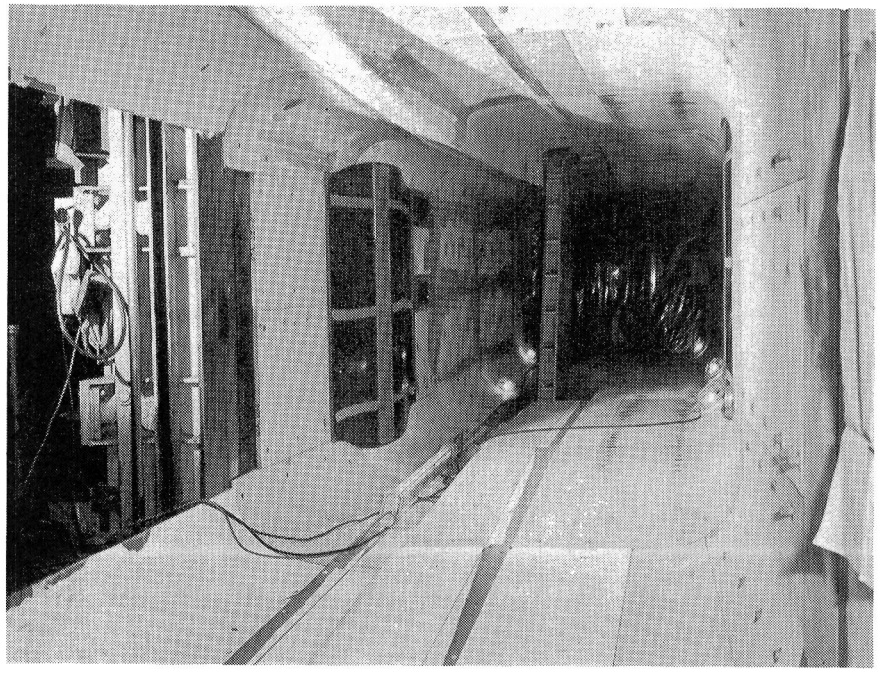

L-81-11,918

(b) Upstream view.

Figure 14. Final design shape for liner diffuser.

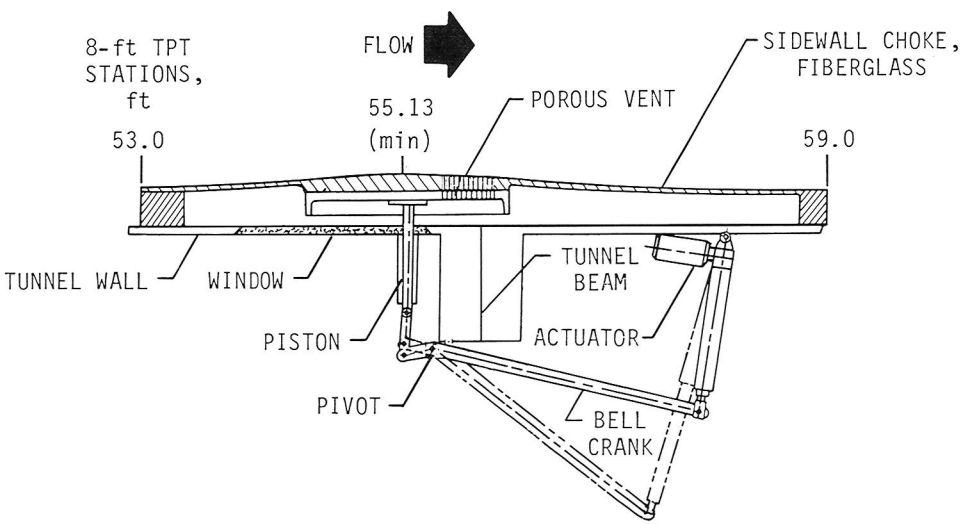

(a) Cross-sectional schematic of choke plate.

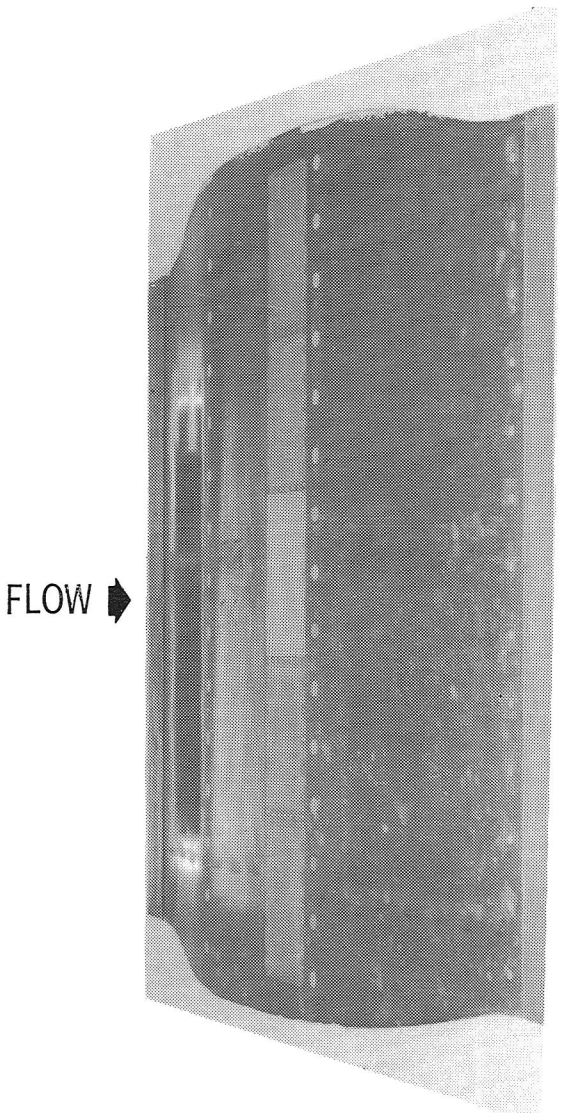

L-82-3071.1

(b) Upstream view.

Figure 15. Some details of remotely controlled, variable-height, tunnel-sidewall choke plate.

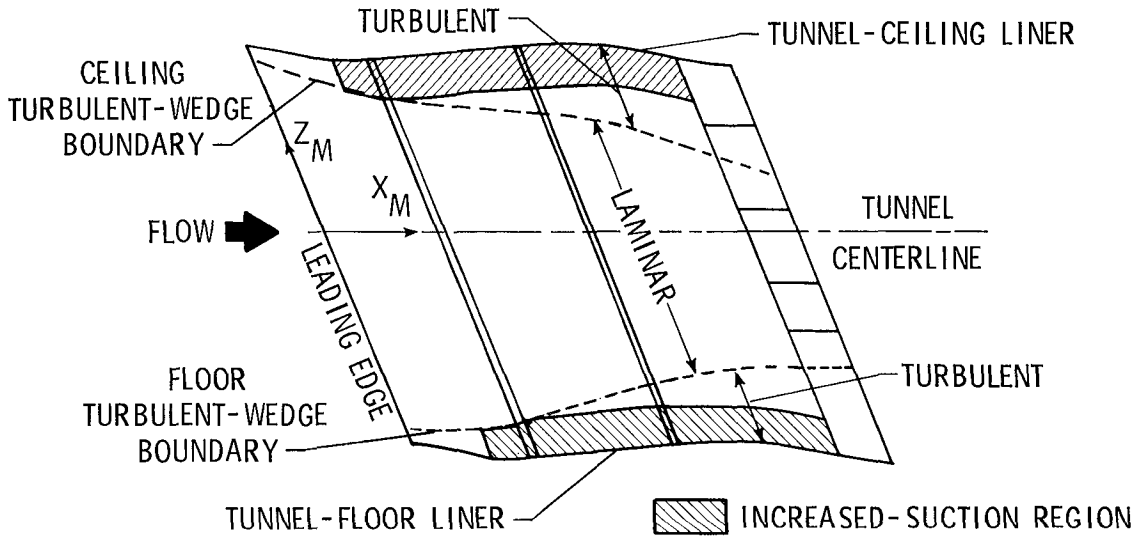

Figure 16. Planform view of turbulent and increased-suction regions on model lower surface.

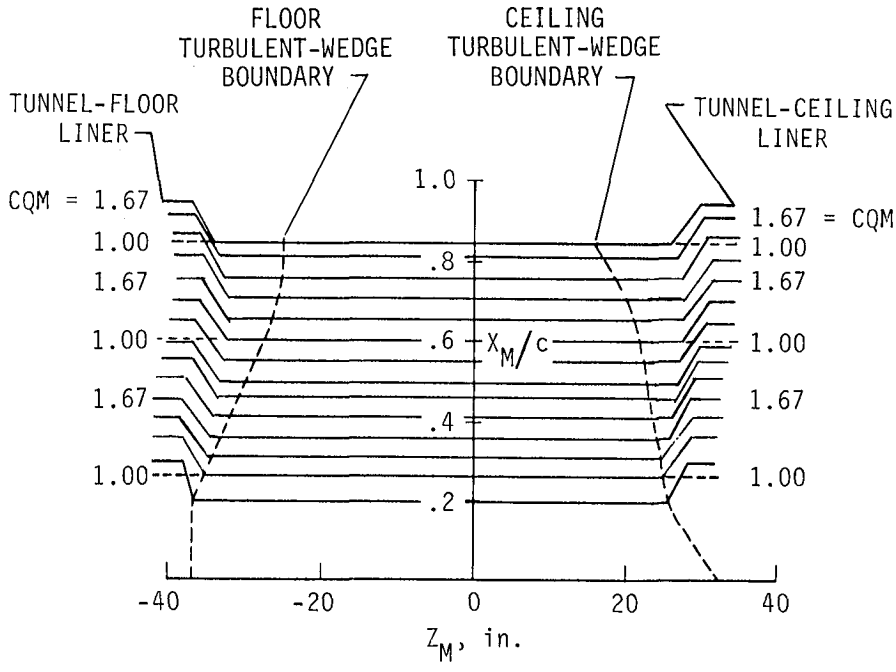

(a) Calculated at design.

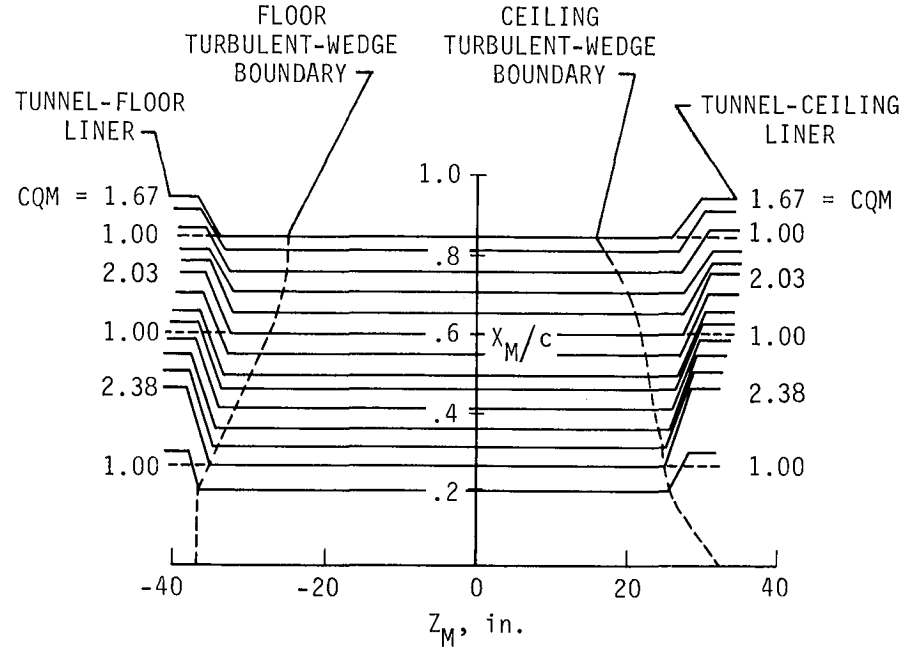

(b) Incorporated in model.

Figure 17. Carpet plots of suction magnification factors in turbulent regions on model lower surface.

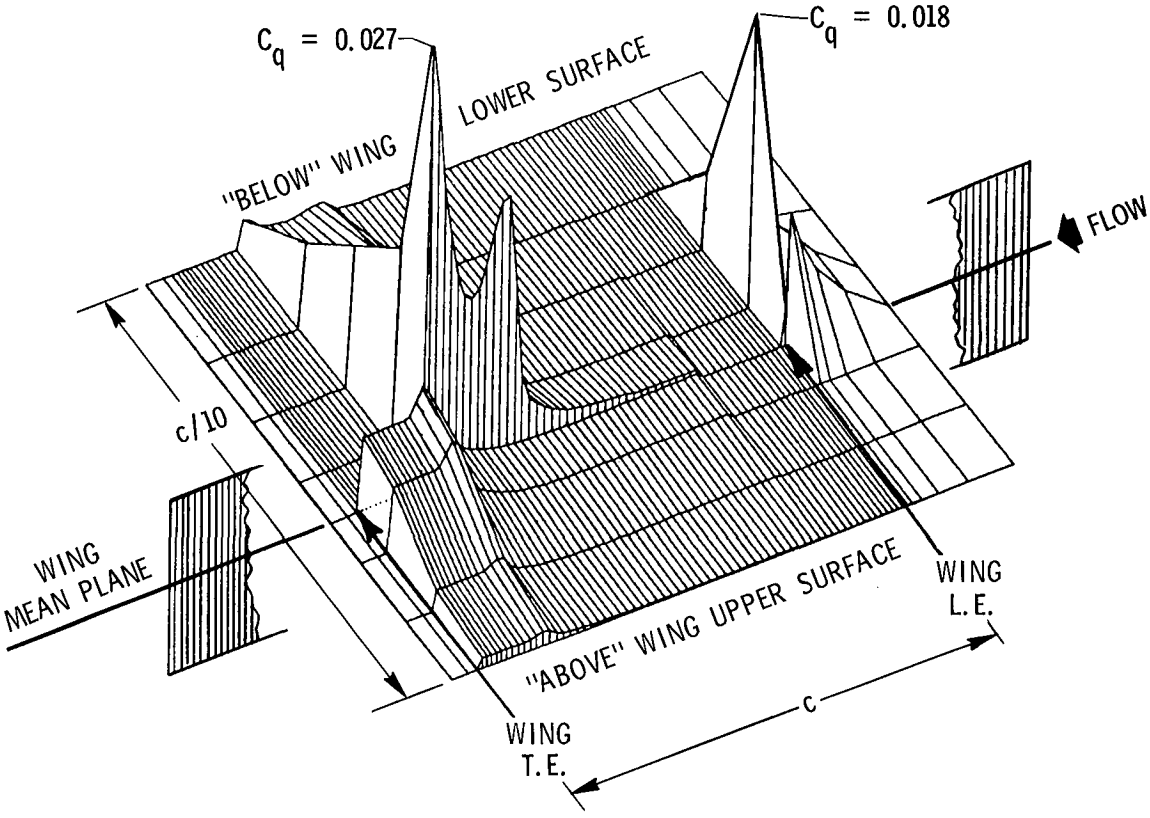

(a) Calculated C_q distribution along streamlines.

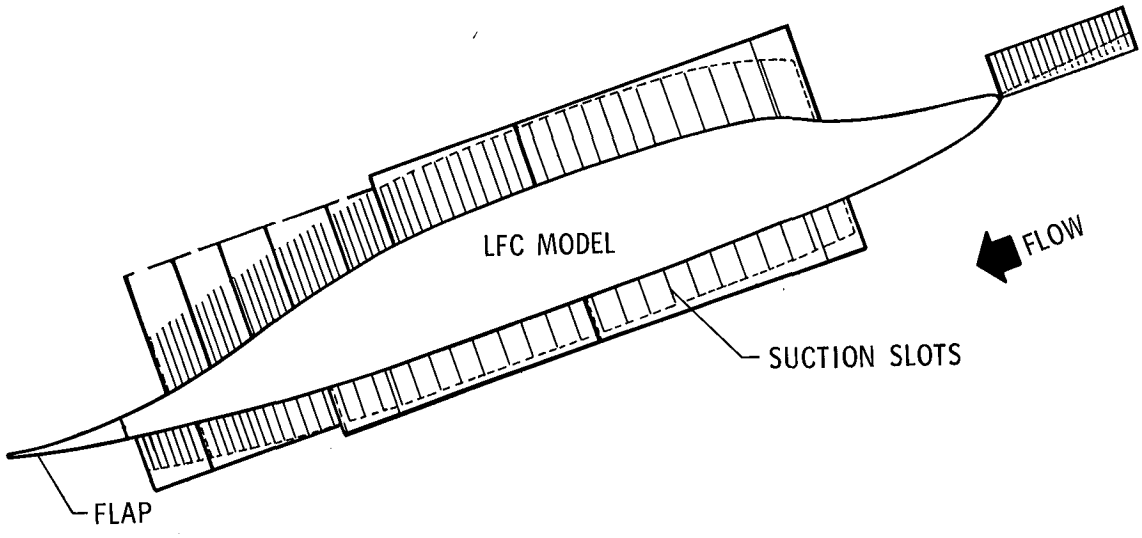

(b) Suction panel-block layout.

Figure 18. Suction distribution and panel-block layout on liner end plate near model at design.

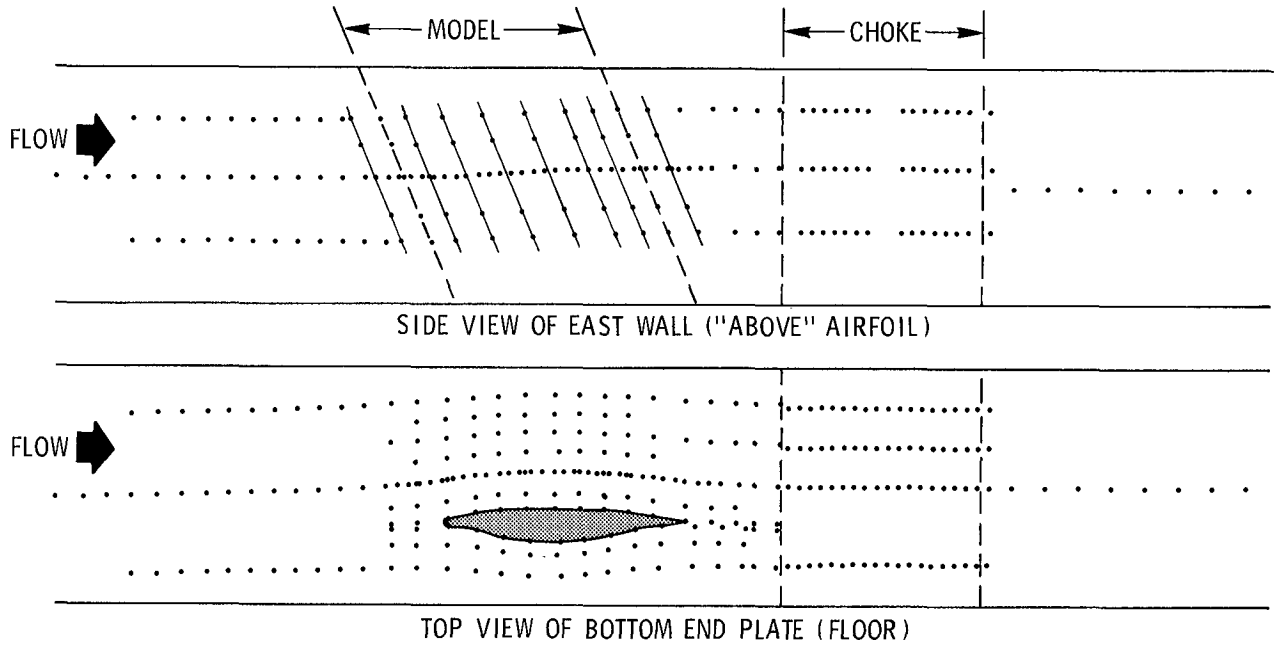

(a) Schematic for pressure-tap locations.

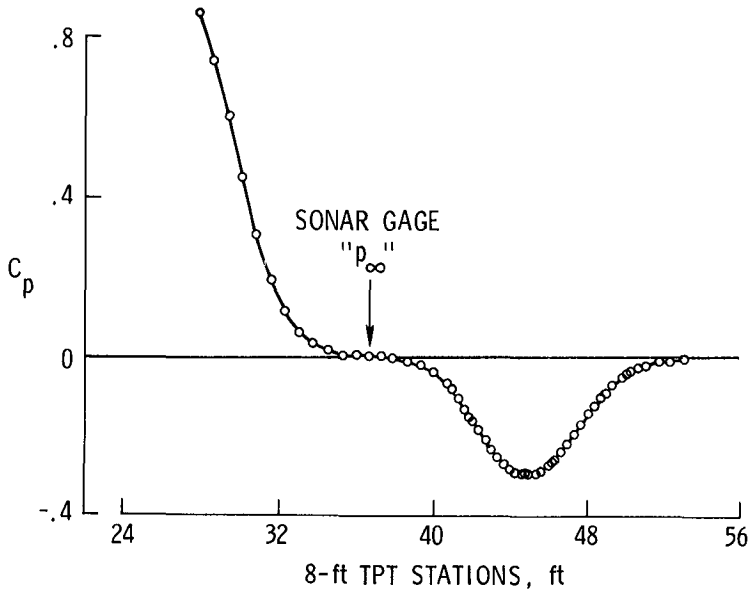

(b) Streamwise distribution of design-point pressure coefficient along middle of liner east wall.

Figure 19. Liner instrumentation and sample pressure distribution at design.

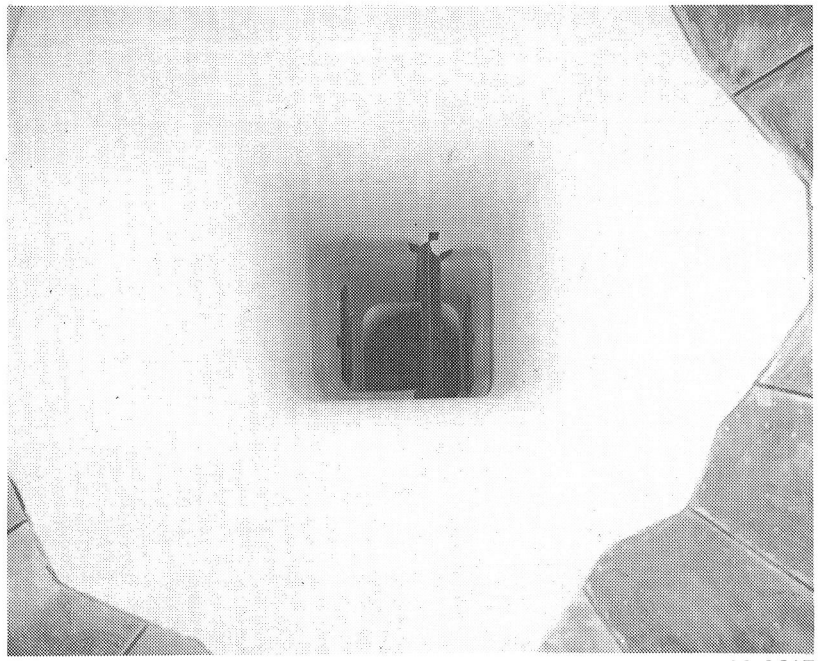

L-82-3617

(a) Downstream view through contraction section.

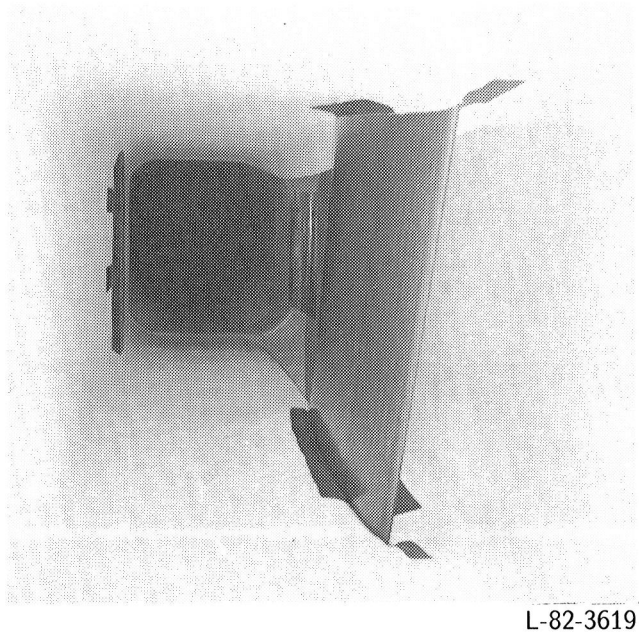

L-82-3619

(b) Downstream view through test section "above" model upper surface.

Figure 20. Finished liner in 8-ft TPT with LFC swept-wing model installed.

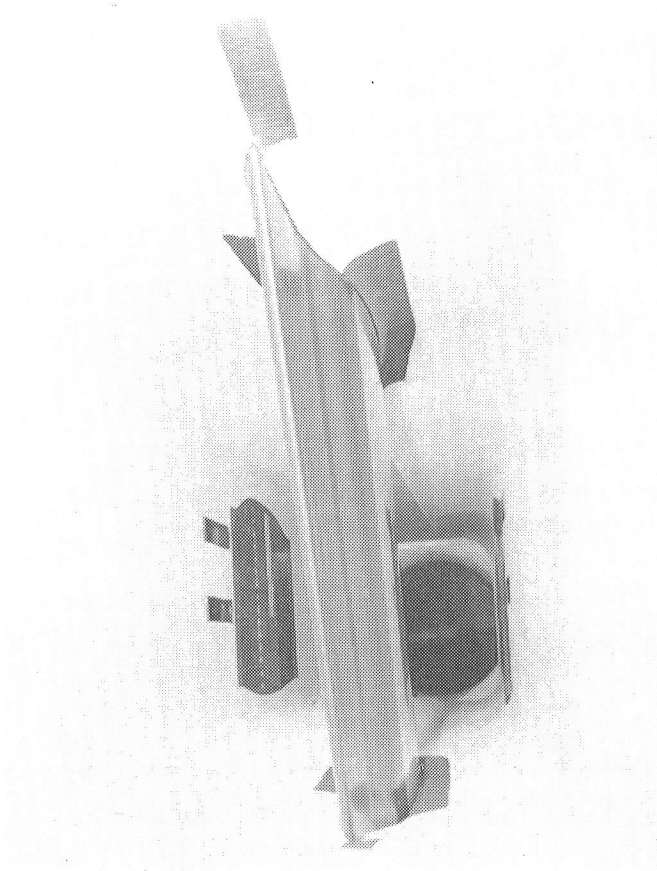

L-82-3070

(c) Downstream view through test section "below" model lower surface.

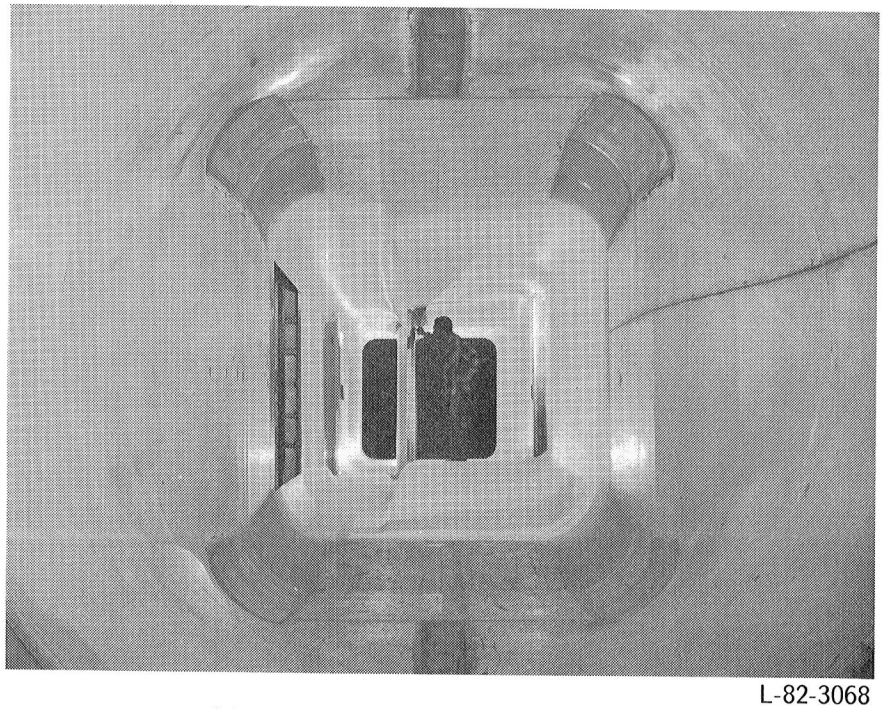

L-82-3068

(d) Upstream view through diffuser section.

Figure 20. Concluded.

1. Report No.	2. Government Accession No.	3. Recipient's Catalog No.
NASA TP-2335		

4. Title and Subtitle	5. Report Date
AERODYNAMIC DESIGN OF THE CONTOURED WIND-TUNNEL LINER FOR THE NASA SUPERCRITICAL, LAMINAR-FLOW-CONTROL, SWEPT-WING EXPERIMENT	September 1984
	6. Performing Organization Code: 505-31-23-06
7. Author(s): Perry A. Newman, E. Clay Anderson, and John B. Peterson, Jr.	8. Performing Organization Report No.: L-15521
9. Performing Organization Name and Address: NASA Langley Research Center, Hampton, VA 23665	10. Work Unit No.
	11. Contract or Grant No.
12. Sponsoring Agency Name and Address: National Aeronautics and Space Administration, Washington, DC 20546	13. Type of Report and Period Covered: Technical Paper
	14. Sponsoring Agency Code

15. Supplementary Notes

This paper is an expanded version of AIAA-82-0568.

16. Abstract

An overview is presented of the entire procedure developed for the aerodynamic design of the contoured wind-tunnel liner for the NASA supercritical, laminar-flow-control (LFC), swept-wing experiment. This numerical design procedure is based upon the simple idea of streamlining and incorporates several existing transonic and boundary-layer analysis codes. The liner, presently installed in the Langley 8-Foot Transonic Pressure Tunnel, is about 54 ft long and extends from within the existing contraction cone, through the test section, and into the diffuser. LFC model testing has begun and preliminary results indicate that the liner is performing as intended. The liner-design results presented in this paper, however, are examples of the calculated requirements and the hardware implementation of them.

17. Key Words (Suggested by Authors(s))	18. Distribution Statement
Laminar-flow control Contoured wind tunnel Transonic flow Supercritical swept wing	Unclassified—Unlimited Subject Category 02

19. Security Classif.(of report)	20. Security Classif.(of this page)	21. No. of Pages	22. Price
Unclassified	Unclassified	46	A03

For sale by the National Technical Information Service, Springfield, Virginia 22161

NASA-Langley, 1984